FEASIBILITY STUDY ON THE INSTALMENT OF WIND TURBINES THROUGHOUT QUEEN MARY UNIVERSITY CAMPUS

By Pelucchi Tommaso

DEN318 Third Year Project (Mech) May 2020

Supervisor: Dr Adrian Briggs

FINAL PROJECT REPORT

SCHOOL OF ENGINEERING AND MATERIALS SCIENCE

ENGINEERING / MATERIALS

THIRD YEAR PROJECT

DEN318

May 2020

DECLARATION

This report entitled

> Feasibility Study on the Instalment of Micro Wind Turbines throughout Queen Mary University Campus

Was composed by me and is based on my own work. Where the work of the others has been used, it is fully acknowledged in the text and in captions to table illustrations. This report has not been submitted for any other qualification.

Name Tommaso Pelucchi

Signed 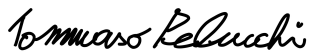

Date 05/05/2020

ABSTRACT:

This report analyses the results obtained from investigating the feasibility of integrating building-mounted wind turbines (BMWTs) within Queen Mary University campus in East London. Analysing this specific case, the aim is also to understand whether urban winds could be profitably used in the future to substantially reduce buildings' electricity costs and CO_2 emissions.

After identifying potential limiting factors of this project, the most suitable buildings for turbines instalment are identified. A Computational Fluid Dynamics (CFD) study of Queen Mary's campus is subsequently completed to understand its wind resource. Improvements to BMWTs locations are then proposed and their potential energy yield is calculated. It is concluded that, by siting turbines high enough on selected rooftops to harvest augmented wind speeds identified through CFD, BMWTs implementation at Queen Mary University is both theoretically feasible and profitable. It is therefore proposed to install 34 turbines over the University's accommodations to reduce up to 38% of their consumptions. Nevertheless, a more in-depth assessment of the site would be required to evaluate rooftops structural performance, study flows from all wind directions and physically measure wind at the site to categorically confirm the feasibility of this project.

List of Contents:

List of Acronyms and Symbols:

Acronym/Symbol	Acronym/Symbol name
A	Turbine's Swept Area (m^2)
AIJ	Architectural institute of Japan
AV	Artificial Viscosity
BMWT	Building Mounted Wind Turbine
CFD	Computational Fluid Dynamics
HAWT	Horizontal Axis Wind Turbine
MWT	Micro Wind Turbine
QM	Queen Mary University of London
SKE	Standard $k-\varepsilon$ model
$\boldsymbol{u}$	Wind speed (m/s)
VAWT	Vertical Axis Wind Turbine
$\boldsymbol{z}$	Height above the ground (m)
Greek Symbols:	**Greek Symbol name**
$\boldsymbol{\rho}$	Density (Kg/m^3)
$\boldsymbol{\alpha}$	Friction coefficient (unitless)

Covid-19 statement:

Due to the circumstances caused by Covid-19, I had to face a series of challenges to readapt my project. As soon as the pandemic broke out, I had just finished setting up all my simulations to be run within the University using ANSYS and Queen Mary's Apocrita HPC (High Performance Computer). Since I was forced to go back to my home country, I stopped using ANSYS, to use a very simplistic online-based CFD tool (Simscale). As it is completely accessible through any web browser, Simscale is the only software that I was able to run on my PC. I also tried running the AppsAnywhere tool provided by the University to use Ansys, however, it was not supported by my computer. Even though some features of Ansys and Simscale are similar, in order to use it properly, I had to completely learn again from scratch how to use this CFD software and recreate all meshes. In addition, I had to learn how to use a different post-processing tool called Paraview to extract data at specific points because Simscale's post-processing tool is extremely limited. This, overall, limited my ability to post-process results. While this provided me with new, interesting skills, it required an extremely high amount of time, also considering that my slow Wi-Fi took at least two hour to download every simulation for post-processing. In addition, Simscale's computational power was limited, which caused me to run simulations much more slowly than expected. Simscale is much more simplified than Ansys, which caused me to have limited mesh generation features and less input parameters. Finally, I aimed to consider more wind directions and more types of wind turbines but was limited both by the core hours limit of Simscale and by time constraints.

1. INTRODUCTION

As world population and quality of life continue to rise, so does the challenge of sustainably keeping up with an electricity demand that is expected to rise until 2040 [1]. In the UK, the Climate Change Act (2008) [2] states that Carbon Dioxide emissions in 2050 have to be at least 80% lower than in 1990. Yang et al. [3] therefore suggests that an "energetic revolution" is required at every scale to exploit all available renewable sources, both in rural and urban areas [3]. Particular attention has therefore been thrown on micro electricity generation, i.e. all methods used by individuals or small businesses to generate electricity within their private spaces, including densely-populated areas [4]. This allows to create a decentralised, low-carbon electricity system, which can decrease costs and emissions of all urban infrastructures, which account for half of the UK CO_2 production [5].

Since the UK is the European country with the best wind resource, Micro wind turbines (MWTs) would play a crucial role for its micro electricity generation [5]. MWTs are vertical (VAWT) or horizontal (HAWT) axis wind turbines with a capacity below 10kW [5]. They can reside on rooftops to exploit higher wind speeds and provide a direct supply of electricity to the building. Yet, the spread of these Building-Mounted Wind Turbines (BMWT) has been limited, mainly due to the slower urban winds and concerns about BMWTs noise and visual impact. In addition, the unplanned patterns of buildings generate wind turbulences that could decrease the available power and produce excessive stresses on turbines' blades [5].

These observations generated a debate on whether BMWTs could become a viable and profitable source of clean electricity for urban environments. Even though several projects proved that BMWTs could bring solid advantages, there are still not enough results and supporting evidence to confirm they could substantially help tackle the increasing energy demand [5]. Furthermore, urban wind speeds, and hence power outputs, are extremely dependent on the surrounding environment and are not yet fully understood. There is therefore an increasing need to study different sites and assess their specific suitability for hosting BMWTs. This project will hence study the overall feasibility of using BMWTs within the university campus of Queen Mary, in Mile End, in the East End of London, where highly electricity-demanding buildings are found. Two different wind turbines are also compared to identify the most suitable for this case.

1.1 AIMS

The overall aim of this project is to consolidate the understanding of and provide clarifications on BMWTs potential in urban environments, while exploring their suitability at a specific site. Clarifying whether this technology could be used to substantially decrease Carbon Dioxide emissions is also important to inspire further studies on this technology. Even though such a feasibility study could have either a positive or negative outcome, the aim would still be to guide potential researchers willing to undertake a similar study and allow the University to understand whether this technology could bring substantial improvements to their specific case.

1.2 PROJECT OBJECTIVES

The first part of this project involves a preliminary research to ensure that the completion of the project could actually benefit Queen Mary University. This involves understanding limiting factors for the instalment of BMWTs at the site and identifying the most suitable buildings for their integration. As urban winds are highly variable, Computational Fluid Dynamics (CFD) simulations have to be performed for multiple wind directions to understand wind's behaviour at the site and propose improvements to the mounting locations. Using CFD results, the potential power output of the whole project using two different turbines are computed and compared with buildings' electricity consumptions. Potential costs savings and the return of investment are also evaluated to ensure the profitability of the project. Taking all findings into account, the feasibility of the overall project should then be assessed to provide specific recommendations for the University.

2. LITERATURE REVIEW

Even though, as mentioned above, the development of BMWTs is still limited, several researchers have tried to understand their potential for urban applications. An in-depth study of the UK current position and potential in the BMWTs industry is provided by Dutton et al. [5]. In their report, major advantages and concerns of integrating turbines within buildings are presented. Their ability to eliminate transmission losses and, when properly positioned, exploit building-augmented winds are presented. Substantial cost savings are particularly predicted when wind power is used to decrease electricity imported from the grid. Drivers for this technology also include the UK government's Climate Change Levy, a tax rated at 0.43 pence/kWh of electricity from non-renewable sources, and UK councils trying to grant more micro generation planning permissions to encourage renewable systems [5].

Dutton et al. [5] and Casini [6] both present issues that are currently limiting this technology, including noise generation, identification of best urban locations and safe operation in turbulent regions. A well-thought comparison of available VAWTs and HAWTs is then completed to conclude that, even though HAWTs, shown in Fig.1, have a higher efficiency, VAWTs are more suited for urban environments. Unlike HAWTs, VAWTs can simultaneously harvest winds from any horizontal direction and hence better cope with the highly variable urban wind directions, which could also induce extreme stresses and noises on HAWTs. Vertical turbines also have their generator on the ground, hence improving ease of access, stability and allowing a more efficient distribution of weights, invaluable for rooftops applications [7].

As shown in Fig.1, there are currently drag and lift types of VAWTs on the market. The first type, called Savonius, exploits wind impacting against its blades to rotate. They are the most reliable turbines but have the lowest efficiencies. All remaining VAWTs have specifically-designed circular (Darrieus turbine), vertical (H-Blade) or curved (Gorlov) blades that create a lift force that drives rotation when wind flows over them [8]. The best turbines for urban applications are either H-Blade or Gorlov types due to their higher efficiency when compared to Savonius types and better reliability compared to Darrieus turbines [8].

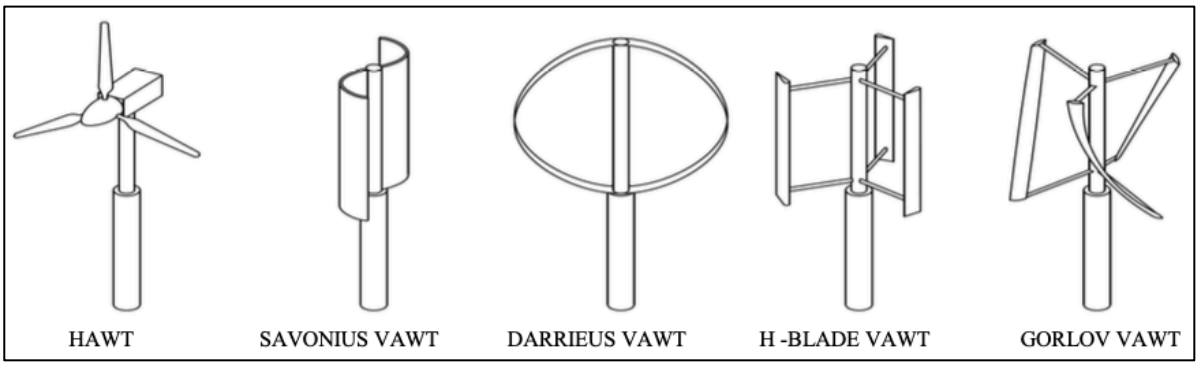

Figure 1: Different types of currently available wind turbines on the market [6]

Other innovative designs are constantly being built and might soon become available. The most remarkable was created by Chong et al. [9], who modified a H-Blade VAWT, shown in Fig.1, using horizontal blades to link the central shaft to the vertical blades, as shown in Fig.2. Noticeable improvements in the power generated and self-starting performance were observed, due to horizontal blades harvesting vertical winds, commonly found in densely built areas. However, as explained by Pelucchi [10], this product is still being developed and there are not yet sufficient data to consider it for power generation studies.

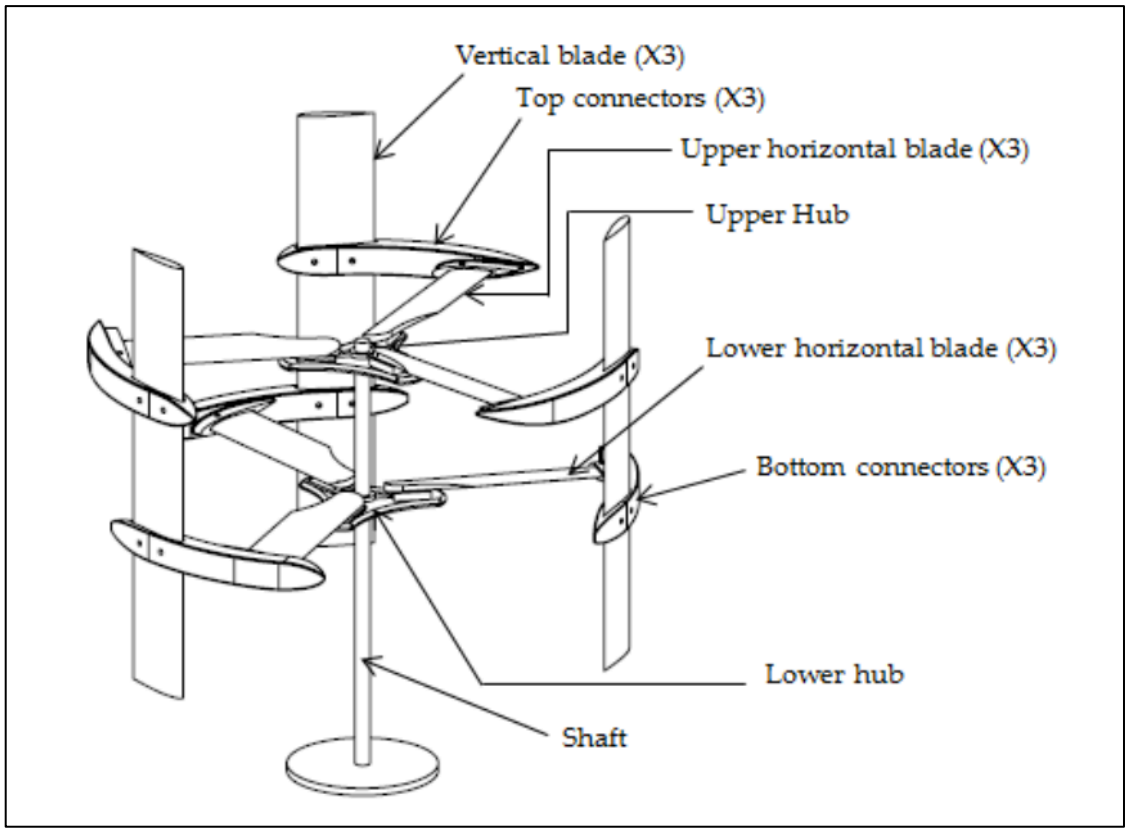

Figure 2: General arrangement of a CAWT [9]

As similar designs are developed, BMWTs will keep improving, increasing their chances of spreading widely. It is therefore crucial to properly evaluate urban flows using CFD with a focus on wind energy exploitation.

2.1 CFD IN THE URBAN ENVIRONMENT

Dutton et al. [5] particularly emphasized that there are not yet enough studies focused on BMWTs urban wind exploitation. In most CFD studies, wind is observed for evaluating Pedestrian Wind Comfort (PWC) or loads on buildings and not, for example, flows over roofs. Both Toja-Silva et al. [11] and Millward-Hopkins et al. [12] therefore underline the need for more CFD analysis of rooftop flows to create a well-established method for their evaluations.

One interesting study conducted by Toja-Silva *et al.* [11] sums up the state-of-the-art of CFD in urban environments to propose turbulence models for urban wind analys. Even though RANS (Reynolds-averaged Navier-Stokes) model cannot deal well with big separation regions, it is one of the most suitable and widely used for urban simulations. Running at least second order accurate simulations, however, RANS can predict very well the behaviour of 'simple' flows with low computational times [13]. LES (Large Eddy Simulation) model, on the other hand, have an excessive computational demand, but provides more accurate simulation results, even

with turbulent flows [11]. Within RANS, the Standard $k-\varepsilon$ (SKE) is the most used eddy viscosity model for urban flows, even though it tends to under-predict turbulences in wake regions [11]. It is generally based on the transport of two quantities, the turbulent kinetic energy (TKE), k and the TKE dissipation rate, ε [13]. Nevertheless, any selected model still has to be rigidly validated against experimental measurements to ensure it accurately represents reality.

As emphasized by Toja-Silva *et al.* [11], a proper mesh is needed to achieve accurate results. Regular, structured elements refined in locations of high flow variations are preferred for urban simulations to avoid excessive artificial viscosity (AV). This viscosity is caused by the software's discretisation of the domain. Even though it is required to ensure the stability of result, it can hardly be spotted, leading to potential errors. Studying increasingly fine meshes, a mesh-converged solution, where the effects of AV are negligible, has to be found [11].

Using this method and the steady RANS SKE model, various results focused on flow over one or a few buildings for energy generation were achieved. Lu and Ip [14] analysed the effects that two separated buildings produce on free-stream flow. A sort of Venturi effect was observed in-between buildings where, if the available space is reduced, wind blows faster, as shown in Fig.3.

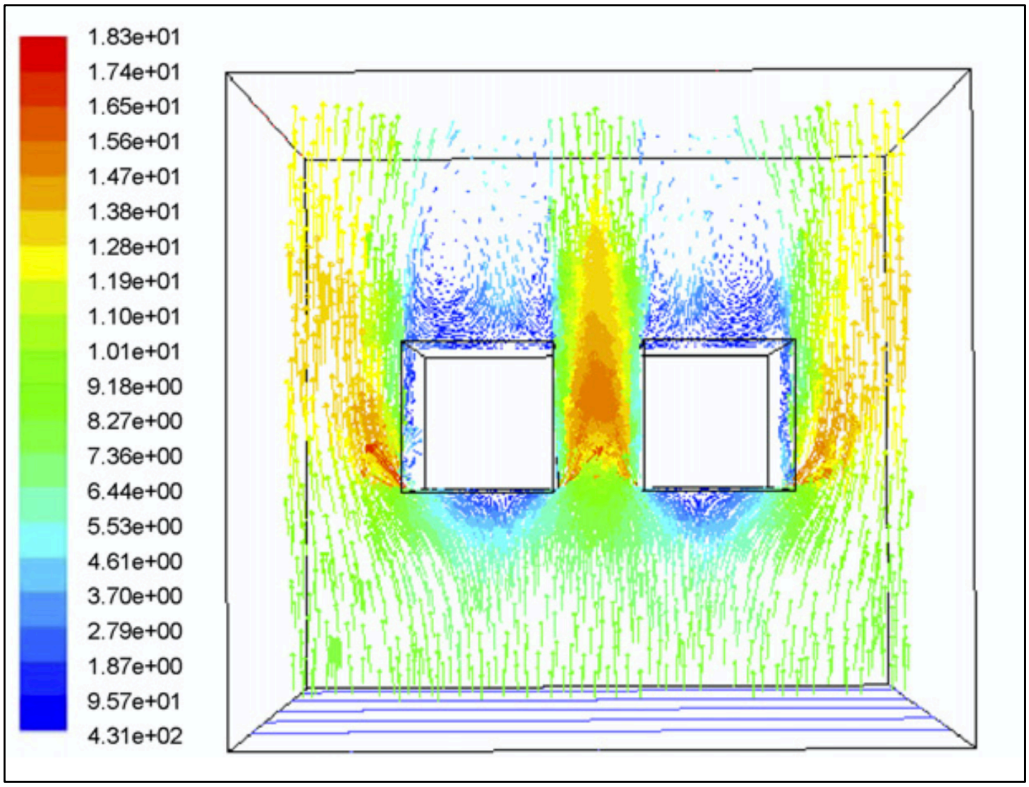

Figure 3: Top view of velocity vectors around two high-rise buildings in free stream (top view) [14]

A similar but less intense acceleration takes place at the sides of the buildings, where a pressure drop allows flow to rotate around the building and hence produces an increase in velocity. According to [14], [15] and [11], buildings' rooftops experience a similar "speed-up" effect, shown in Fig.4, which could lead to 3 times higher power generated than at free stream. An additional increase in velocity was noticed on the roof surface, caused by recirculating flow.

Superimposing HAWTs and VAWTs on their CFD results, as shown in Fig.4, Toja-Silva *et al.* [11] observed that, if turbines can't be placed above the recirculating zone, HAWTs would be impractical. Wind flowing in the opposite direction would strike again on their blades, generating an opposite force leading to potentially dangerous, sudden ruptures. VAWTs, however, would still function properly as they would harvest recirculating winds to further increase their rotational speed.

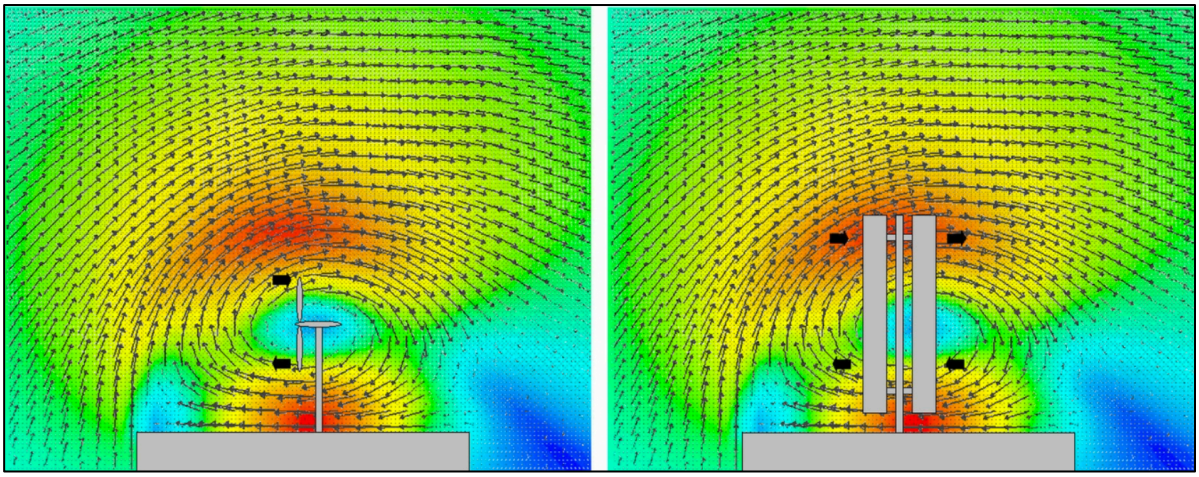

Figure 4: Superimposition of an HAWT and VAWT over wind flow on a flat roof [11].

The above is just one example showing how CFD can be useful to avoid unsuitable choices and maximise turbines' performance. Further research on larger arrays of buildings has been carried out by Heath et al. [16], who demonstrated that, even when surrounding houses have roughly similar heights, their influence on the flow is substantial and could highly decrease overall wind speeds. However, since there are not many other studies analysing flow over buildings blocks, it is still hard to properly confirm the existence of easily identifiable, recurrent urban patterns. Therefore, the specific assessment of each potential site still has to be evaluated using CFD.

Overall, there are also not enough projects that study specific sites and try to calculate potential power outputs, comparing them with buildings' consumptions to ensure the profitability of installing BMWTs. This lack of supporting information is still widely enhancing debates on

BMWTs usage and profitability. It is hence necessary to analyse as many specific cases as possible and provide tangible evidence on their suitability for urban wind exploitation, as presented in the following sections of this report. Before, however, it is crucial to understand how the available wind power in urban areas is calculated when using CFD simulations.

2.2 WIND POWER EVALUATION IN URBAN AREAS

The theoretical method to evaluate turbines power output assumes that their power curve ($P_{output}(u)$), which expresses the turbine's power output at each wind speeds u, is known [4]. Furthermore, the probability density function (PDF), $f(u)$, representing the frequency with which every speed u is measured at the site is required [4]. The average turbine power output can then be calculated integrating between the minimum and maximum velocities [4]:

$$\bar{P}_{turbine} = \int_{u_{min}}^{u_{max}} P_{output}(u) \cdot f(u) du \qquad 1$$

However, the power curve is often not known. Furthermore, when velocities are obtained from CFD simulations and not from yearly measurements, the frequency with which wind speed occurs at each point cannot be evaluated. Therefore, simulations often assume that wind's probability over one year at all points varies following a known curve called Rayleigh distribution, which fits extremely well with experimental data, even in urban locations, as confirmed by Ouahabi et al. [17]. Using input parameters for CFD simulations based on yearly averages and evaluating velocities at steady state conditions, this assumption allows to calculate average turbines' output at any point using Eq.2, where $\bar{u}$ is the velocity extracted from CFD simulations. The turbine's rotor efficiency, C_p, accounts for the fraction of wind power extracted from the wind by the turbine [4].

$$\bar{P}_{turbine} = \frac{6}{\pi} \cdot 0.5 \cdot \rho \cdot A \cdot \bar{u}^3 \cdot C_p \qquad 2$$

Other efficiencies can also be included in Eq.2 to account for mechanical, electrical or wake losses (occurring when multiple turbines are located at the same site). After analysing all possible wind directions, i, using CFD, the final equation to compute the annual electricity production, E is:

$$E = \sum \bar{P}_{turbine,i} \cdot t_i \qquad 3$$

Where t_i is the total annual time at each wind direction i.

When the power curve of a turbine is available, however, the power output at $\bar{u}$ for all wind directions can be directly read from the graph provided by the manufacturer. Once again, Eq.3 can be used to evaluate the annual electricity output.

The following sections will now outline all the steps followed to evaluate the feasibility of installing BMWTs within Queen Mary University's campus and eventually exploit CFD simulations to compute potential energy savings.

3. PRELIMINARY INVESTIGATION

The first step helped making sure that Queen Mary University would take this project into consideration in case of a positive outcome. Using consumptions data provided by the University' Sustainability team, 80% of its CO_2 emissions were found to be due to electricity. Since QM University aims at creating "a built environment that meets high environmental performance standards" [18], cutting electricity consumptions using BMWTs would help it achieve this goal, reducing its environmental impact.

Before proceeding further, the approximate potential energy yield was calculated using yearly wind data at 10m height, starting from 11/03/19, provided by Meteoblue.com [19] for the University's exact location (51.53°N 0.04°W). These raw data are shown in Sec.1 of the Appendix and graphically presented in the wind rose inFig.5, where it is clear that wind comes predominantly from south-west or west with maximum speeds between $12m/s$ and $14m/s$. Using these data, the overall average velocity $\bar{u}$ at the site was calculate as:

$$\bar{u} = \sum_{u=0}^{u=uf} u \cdot \frac{t_u}{t_y} = 3.3m/s \qquad 4$$

where $t_u =$ total hours at velocity u; $t_y =$ total hours in one year $= 8760$ hours. Assuming wind varies following the power law shown in Eq.5 [20], wind speed at $z = 20m$, i.e. where most BMWTs are placed, was calculated as shown in Eq.6:

$$u(z) = u(z_r) \cdot \left(\frac{z}{z_r}\right)^{\alpha} \qquad 5$$

Where $\alpha =$ friction coefficient $= 0.28$ and $z_r =$ reference height $= 10m$ [20],

$$u(z) = 3.3 \cdot \left(\frac{20}{10}\right)^{0.28} = 4m/s \qquad 6$$

Using Eq.2 and considering a VAWT with a 4x4m rotor and a C_p =35%, the annual electricity produced per turbine is:

$$E = \frac{6}{\pi} \cdot 0.5 \cdot \rho \cdot A \cdot \bar{u}^3 \cdot C_p \cdot \left(\frac{number\ of\ hours}{year}\right) = \quad (7)$$

$$= \frac{6}{\pi} \cdot 0.5 \cdot 1.225 \cdot (16m^2) \cdot \left(\frac{4m}{s}\right)^3 \cdot 0.35 \cdot (8760) = 3{,}673kWh \quad (8)$$

Compared with solar panels recently installed by the University on its library, producing 30,000kWh per year, one turbine could potentially produce about 12.2% of this amount. Using multiple BMWTs simultaneously and exploiting speed-up effects over roofs, this technology could hence produce competitive, interesting amounts of electricity for the University.

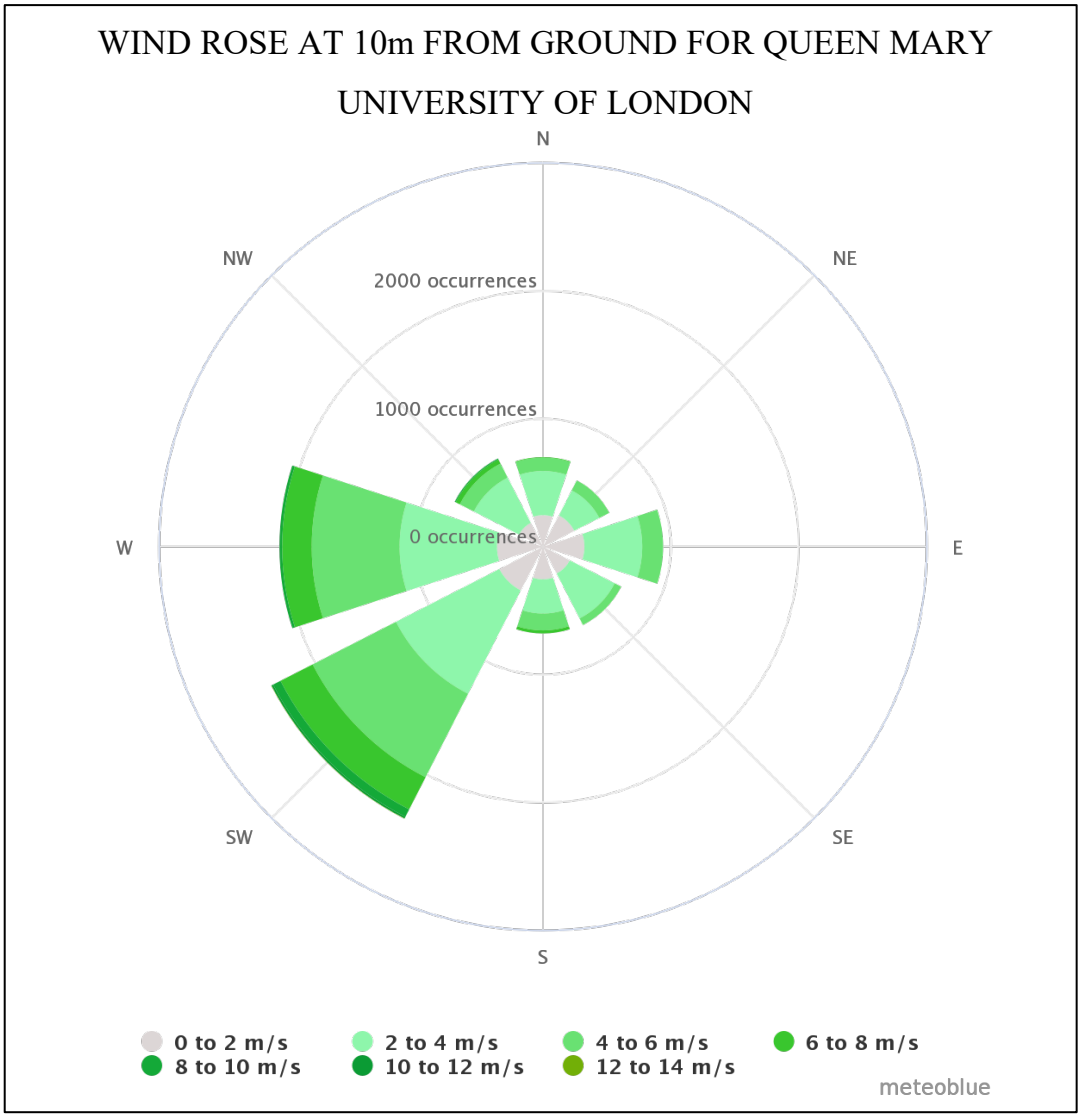

Figure 5: Wind rose at 10m height for QM University East London Campus [19]

To analyse legal constraints, the local council Tower Hamlets was contacted since current UK regulations state it is their responsibility to fully assess the project and potentially grant planning permissions. The council appeared prone to permit similar sustainable projects, only provided that safety is guaranteed, noise levels remain within limits and both impacts on wildlife and on the environment's aesthetic are minimised (Chris Blandford, 2017).

These two initial outcomes were sufficient to partially confirm the feasibility of the project and justify a research of the most suitable sites for BMWTs, as shown in the following section.

4. RESEARCH OF BEST LOCATIONS FOR BMWTs

Using the recently-updated Tower Hamlet's 2031 Map, shown in Fig.6, all University buildings were identified and highlighted in red. Listed Buildings and Parks, coloured respectively in light green and green in Fig.8 were then discarded as they are historically important sites where no developments are permitted [21]. Finally, to ensure the easiest implementation and operation

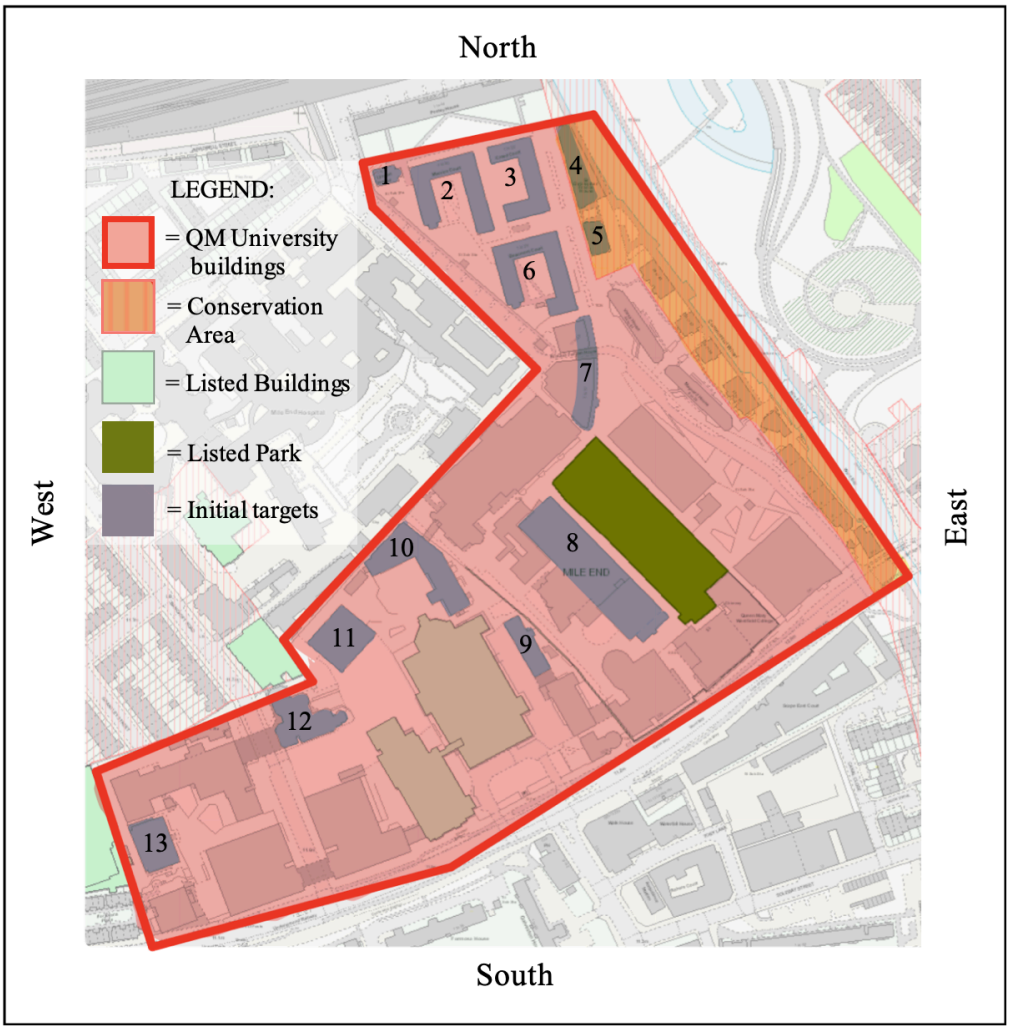

Figure 6: Tower Hamlet's 2031 Local Plan Map used to identify suitable locations for BMWTs [26].

of turbines, flat, accessible roofs were identified, highlighted in blue and numbered in Fig.6. Buildings 8 and 11 were then discarded as the University is planning to respectively demolish and renovate them. All buildings' real names can be clearly seen in Sec.2 of the Appendix.

Selecting a group of nearby buildings would allow to achieve more accurate CFD predictions and facilitate installation of BMWTs, hence two potential sites were identified. The first includes buildings 1 to 7, i.e. all University's accommodations, while the second one comprises buildings 9, 10, 12 and 13. Since the second group has much further buildings and lower roof sizes, buildings 1 to 7 were chosen for this study. These buildings are also relatively new and have no refurbishment plans, allowing installation of BMWTs for at least 20 years, i.e. their average lifetime [5]. Since buildings 4,5 are in conservation areas, i.e. where any new construction must enhance the character and appearance of the area [21], careful consideration has to be taken when choosing turbines for the site.

Further motivations to select these target buildings were found observing their consumption data for 2018/19. It was observed that these are highly consuming buildings where no electricity comes from renewable sources. Furthermore, their daily consumptions and wind availability over one day were found to have compatible trends, as shown in Fig.7, where electricity demand for France House (Buildings 4,5) is compared to the hourly wind speed available [19].

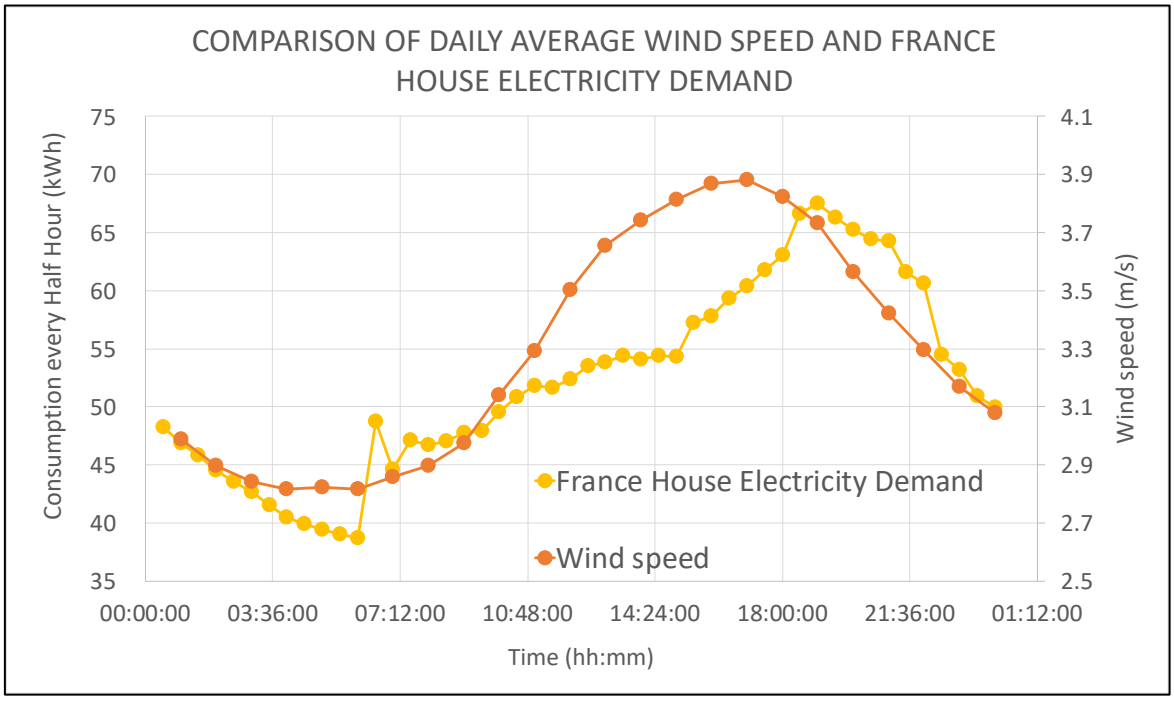

Figure 7: Comparison between wind availability and France House (Buildings 4,5) electricity consumption within a day

This suggests that there are considerable chances to use the produced electricity directly within the building at any time of the day, without storing it in additional batteries. A similar but less pronounced match was observed comparing electricity demand and wind availability over an entire year.

Having found some suitable buildings for BMWTs, the following sections present the CFD analyses completed to study wind flows in this region.

5. CFD MODELLING OF WIND FLOW

To accurately simulate wind flow over the target area of Queen Mary University, a strict validation of the simulation parameters was completed using a benchmark case study.

5.1 BENCHMARK CASE STUDY FOR VALIDATION

Even though the fully detailed procedure used for validation is shown in Sec.3 in the Appendix, this section presents the major findings and parameters used.

The geometry exploited is a simplified urban configuration, shown in Fig.8(a), for which experimental data are provided by the Architectural Institute of Japan (AIJ). It consists of nine scaled-down cuboid buildings with side lengths $D = 0.2m$ (AIJ, 2016), where velocity was measured at the 120 points shown in Fig.8(b).

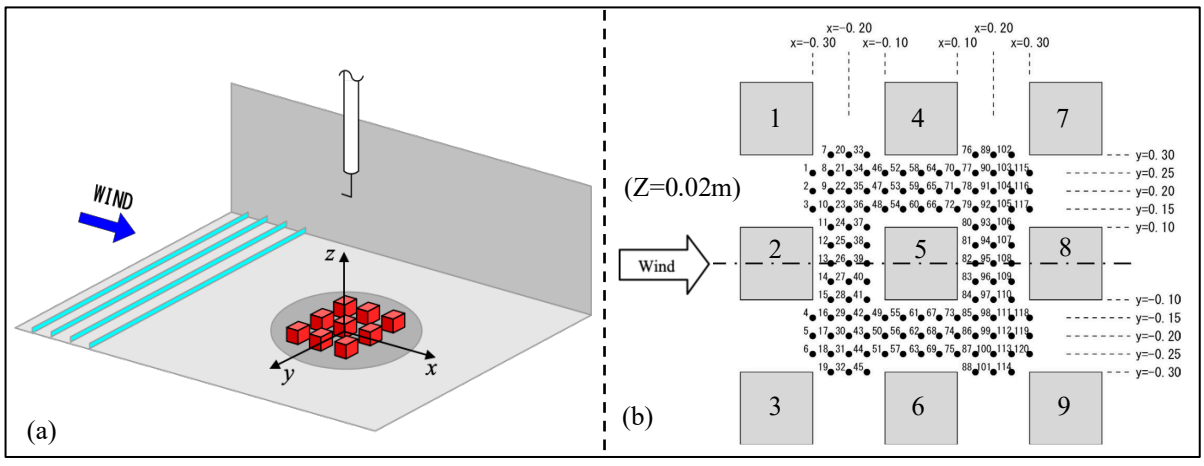

Figure 8: AIJ's experimental setting (a) used to evaluate velocities at all black points (b) (AIJ, 2016)

The major parameters validated here include fixed density ($\rho = 1.225\ kg/m^3$) and viscosity ($\upsilon = 529m^2/s$), the mesh, turbulent model and initial (IC) and boundary (BC) conditions.

As suggested by the AIJ (2016), the inflow wind profile was approximated using Eq.5, where $\alpha = 0.28, z_r = 0.15m, u(0.15m) = 3.48m/s$. The inlet profile can therefore be seen in Fig.9.

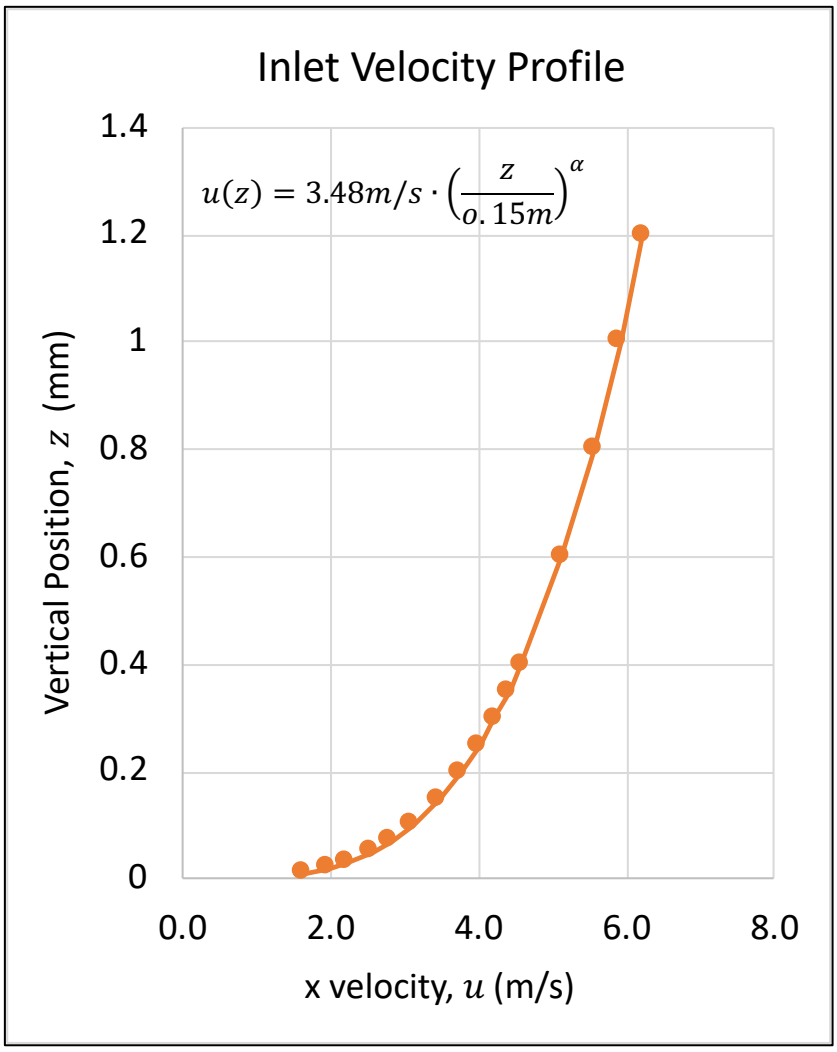

Figure 9: Inflow power law boundary condition for benchmark validation case

At the outlet, the BC is gauge pressure $= 0\ Pa$ to allow velocities to adjust freely depending on what happens in the domain. Since all remaining boundaries are solid surfaces, they are modelled using the Wall No-Slip BC. As suggested in Sec.2, second order accurate simulations are run using the steady RANS SKE turbulence model to look for the steady state solution within reasonable times. The initial flow condition selected was: $u_x = 3\ m/s$.

Having arranged the simulation, a lengthy trial and error approach, presented in Sec.3.2 in the Appendix, was now completed to find the most suitable mesh. Factors like skewness (elements angles should be less than 120°), regularity (opposite sides of cells should be as parallel as possible) and smoothness (variations of elements size should occur gradually) were all

considered [13]. The final mesh has structured, quadrilateral elements and the three refinements as shown in Fig.10,11.

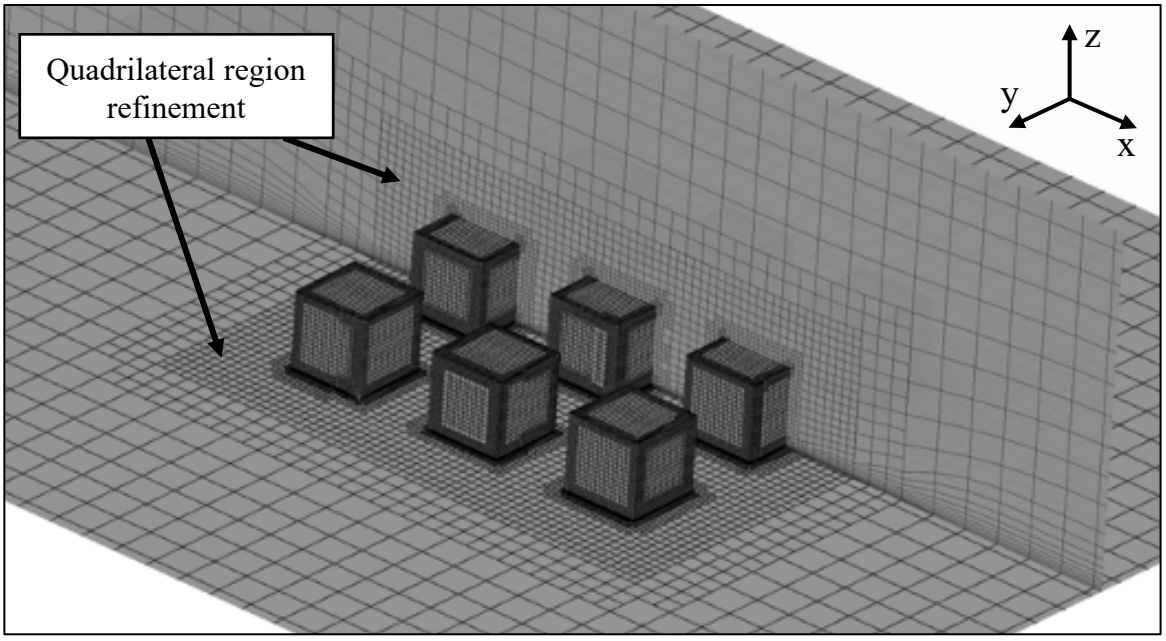

Figure 10: Mesh layout generated to run the benchmark case study showing a region refinement

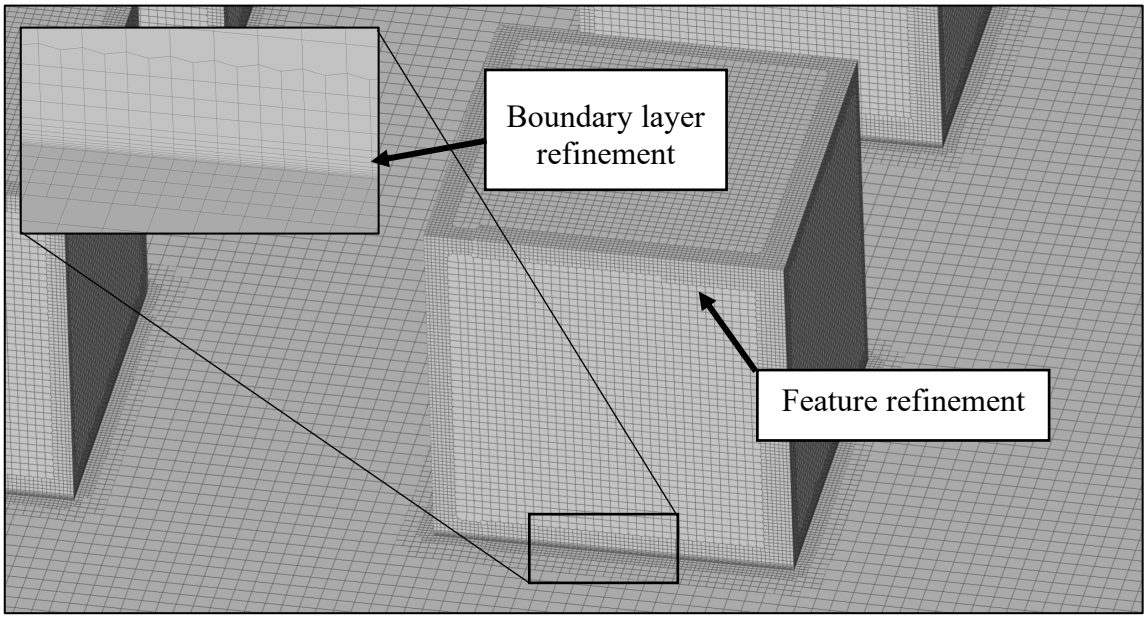

Figure 11: Details of one cube of the selected mesh showing the feature and boundary layer refinements selected to run the benchmark study

Using these mesh parameters, three increasingly fine meshes were tested and compared against wind tunnel measurements. After making simulations converge in time by ensuring residuals (rate of change of a quantity in each cell) tended to zero, mesh convergence was confirmed by

noting that the results of the medium and fine mesh were only slightly different and tended towards the experimental data, especially in non-turbulent regions, as shown in Fig.12

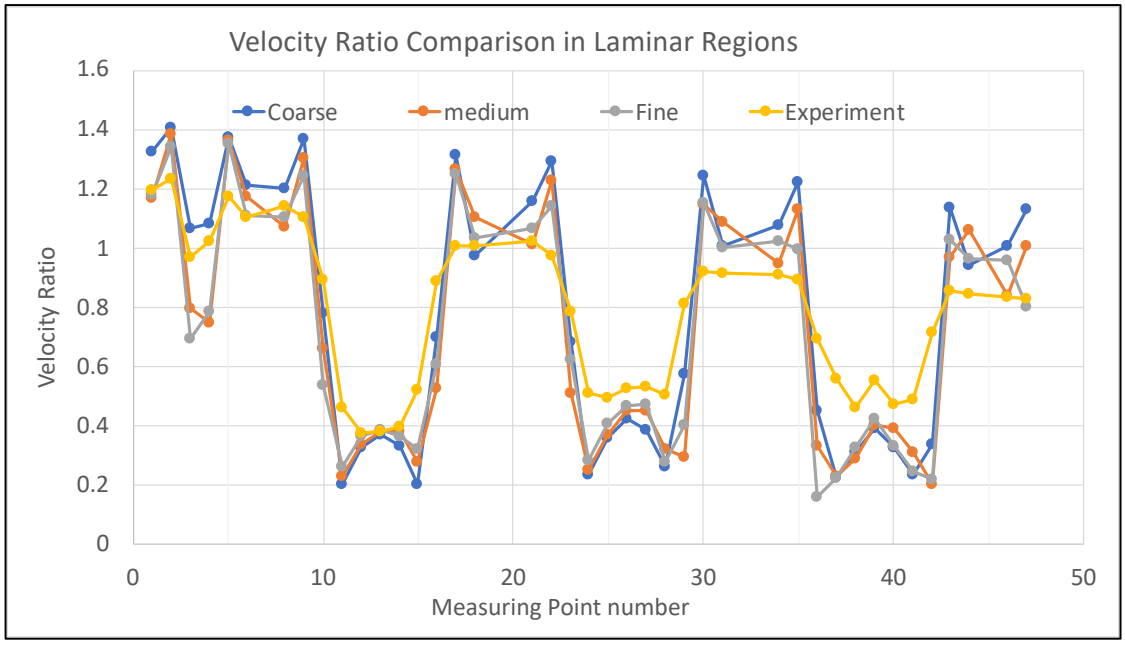

Figure 12: Comparison of velocity ratio obtained from simulations and experimental data in laminar regions

Even though such a similar match with experimental data was not observed in extremely turbulent regions, the overall error of the finest simulation was found to be only 30%. Validation of the model was therefore confirmed, reminding that flow in laminar regions is much better predicted, compared to turbulent regions, where high errors could still take place. This behaviour of the steady RANS SKE model was however predicted in Sec. 2.1 and will have to be considered when analysing wind flows over Queen Mary University.

5.2 QUEEN MARY UNIVERSITY'S CFD SIMULATIONS

Having validated the above case, flow over the University was then analysed by changing only a few parameters to run this specific case as closely to reality as possible.

5.2.1 SIMULATIONS SETUP

The first difference is the 3D CAD model, shown in Fig.13, created using the Fusion 360 CAD Software and dimensions provided by QM Estates and Facilities department. As shown in Fig.13, the model now includes the University's target buildings, highlighted in green, and all constructions closer than $6 \cdot H$, where H is each building's maximum height [23]. Apple's map (2020) is also shown to better locate the target buildings.

Figure 13: 3D CAD Geometry of the University created using Fusion 360 and used in this study

Following the COST 732 guidelines for CFD [23], the vertical extension of the computational domain from the tallest building, having maximum height H_{max}, was set as $8 \cdot H_{max}$. Upstream, the distance between inlet and the first building was $7.5 \cdot H_{max}$, downstream $5 \cdot H_{max}$ while, laterally, it was $5 \cdot H_{max}$ from the buildings block. Dimensions of the domain for the south-west case are shown in Fig.14 while, those for all other simulations are in Sec.4 of the Appendix.

Boundary conditions of the sides and top were set as 'slip', since we are not considering a wind tunnel flow anymore, while the outlet BC was kept as zero static pressure. The inlet BC was created using again Eq.5, where $\alpha = 0.4$ to simulate the atmospheric boundary layer found in cities [20] and $u(z_r)$ was calculated differently for each direction using data from the wind rose of Fig.5. Ideally, all wind directions should be simulated but, in this project, only the three most recurrent directions were tested (SW, W and E). The three inlet profiles are therefore:

$$\text{SW: } u(z) = (3.987m/s)\left(\frac{z}{(10m)}\right)^{0.4} \quad 8$$

$$\text{W: } u(z) = (3.827m/s)\left(\frac{z}{(10m)}\right)^{0.4} \quad 9$$

$$\text{E: } u(z) = (2.657m/s)\left(\frac{z}{(10m)}\right)^{0.4} \quad 10$$

All remaining parameters remained the same as before and have been represented in Table 1.

Table 1:Major settings used to simulate wind flow over Queen Mary University

Turbulence Model	Algorithm	Eddy viscosity model	Density (Kg/m^3)	Viscosity (m^2/s))	Initial condition
Steady RANS	SIMPLE	Standard $k-\varepsilon$	1.1965	1.529	$u_x = 3\ m/s$

Once again, three increasingly fine meshes were created using the parameters presented in Fig.10,11, with the difference that the region refinement is now a cylinder to better fit the new geometry. These features can all be seen in Fig.14,15 where the medium mesh used for south-west simulations is shown. Wind is always assumed to blow from the negative to the positive x direction.

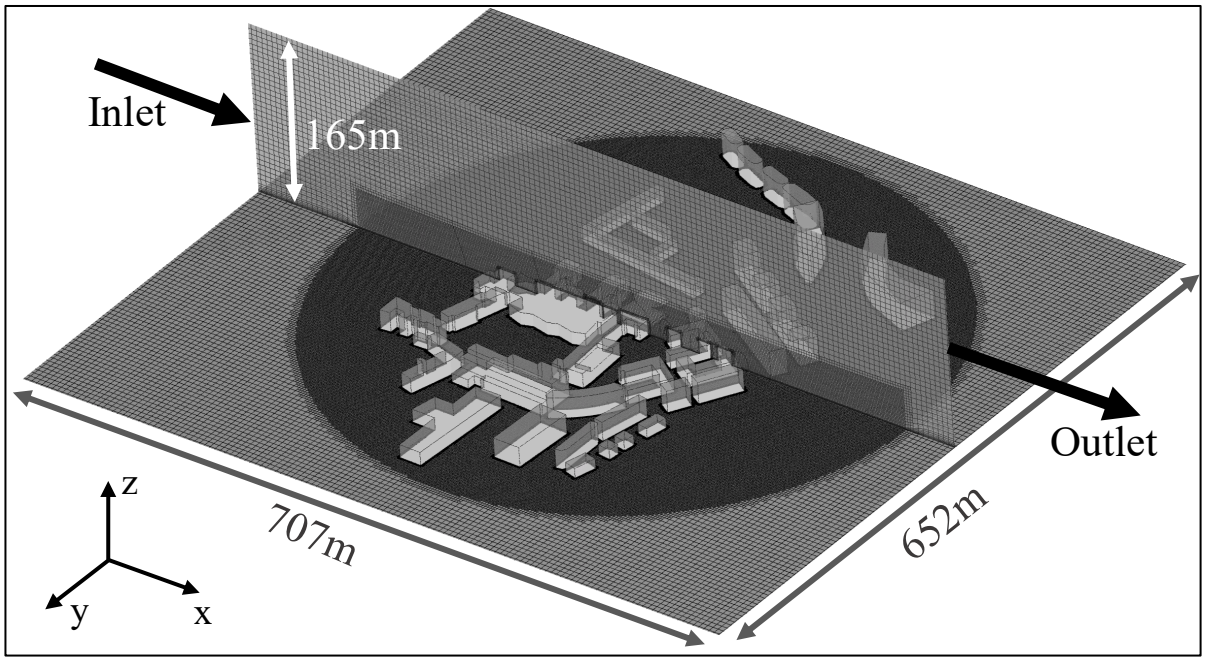

Figure 14: Representation of the medium mesh used for south-west simulations

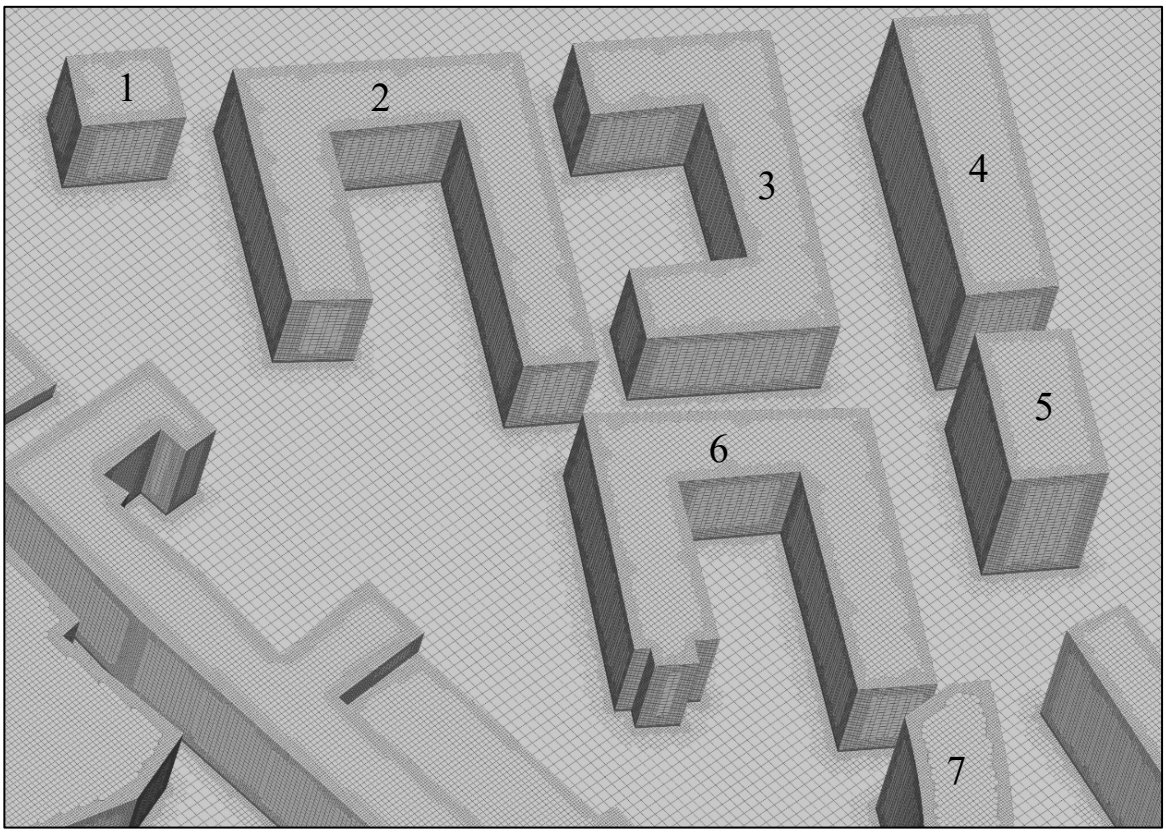

Figure 15: Highlight of the medium mesh generated for Queen Mary University's simulations

5.2.2 SIMULATIONS TIME AND MESH CONVERGENCE

Three increasingly fine meshes were created for each wind direction and tested accordingly. The number of elements in each coarse, medium or fine mesh were all very similar and are shown in Table7 in the Appendix.

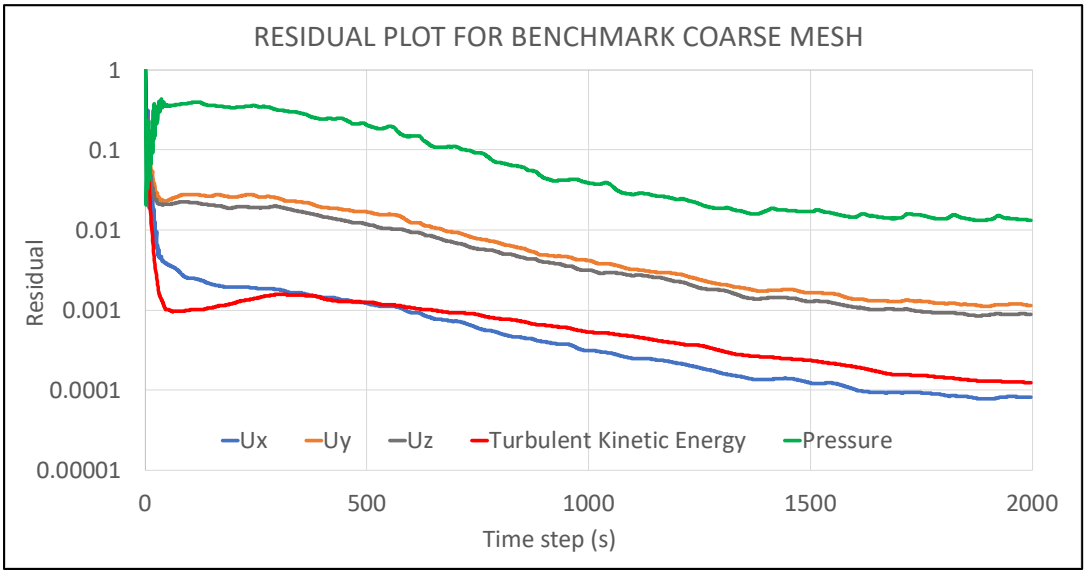

Figure 16: Convergence plot showing the residual of velocities, pressure and TKE

All simulations were run making sure that time convergence was achieved. A typical converged plot is shown in Fig.16, where a logarithmic scale is used. Even though the residual of pressure remains quite high, those for velocities, which is our main focus, tend to zero more noticeably, reaching values between 0.0001 and 0.001.

Convergence was always further confirmed by monitoring variations of the x, y and z velocity components at specific points over target buildings to ensure that, if simulations were run further, results would have not changed. Mesh convergence was then analysed by extracting velocity magnitudes at even more target points and comparing values obtained using the three meshes. These data were then plotted in Fig.17, where velocities at 29 points for the south-west simulations are compared. It is clear that values are extremely similar at most points. Whenever discrepancies are observed, the medium and fine values are always much closer than the medium and coarse, meaning that mesh convergence is being closely approached. Noticing that the overall error between fine and medium meshes was just 3%, mesh convergence of the finest mesh can be confirmed.

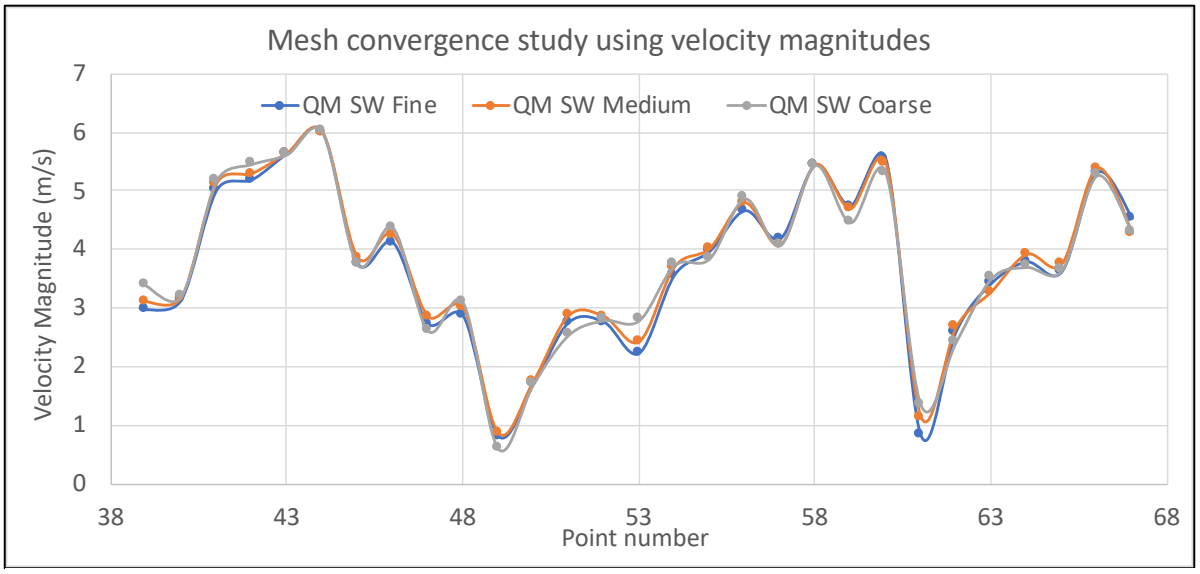

Figure 17: Mesh convergence analysis of Queen Mary University's south-west simulations

5.2.2 SIMULATIONS RESULTS (SW, W, E DIRECTIONS)

Having confirmed mesh and time convergence of all simulations, the finest meshes were used to analyse flows and identify the best wind conditions for turbines. Throughout this analysis, it was assumed that turbines are generally mounted on 6m towers above buildings [11], furthermore, all velocity fields shown in Fig.18,19,20 were created using the same velocity scale shown in Fig.18.

Similar wind patterns above rooftops were observed for all three directions. A noticeable speed-up effect occurs on the first roofs hit by the wind above the recirculation zone. Such an effect is noticeable on buildings 4,5,7 when wind blows from east. In these cases, the augmentation was more enhanced on the western side of the roof, as shown in Fig.18. Since the recirculation region remains below 6m, it is possible to position turbines on the western edge of the building and exploit this local increase in wind speed, as shown in Fig.18. Wind speed here was found to be always at least 1m/s faster than at free stream.

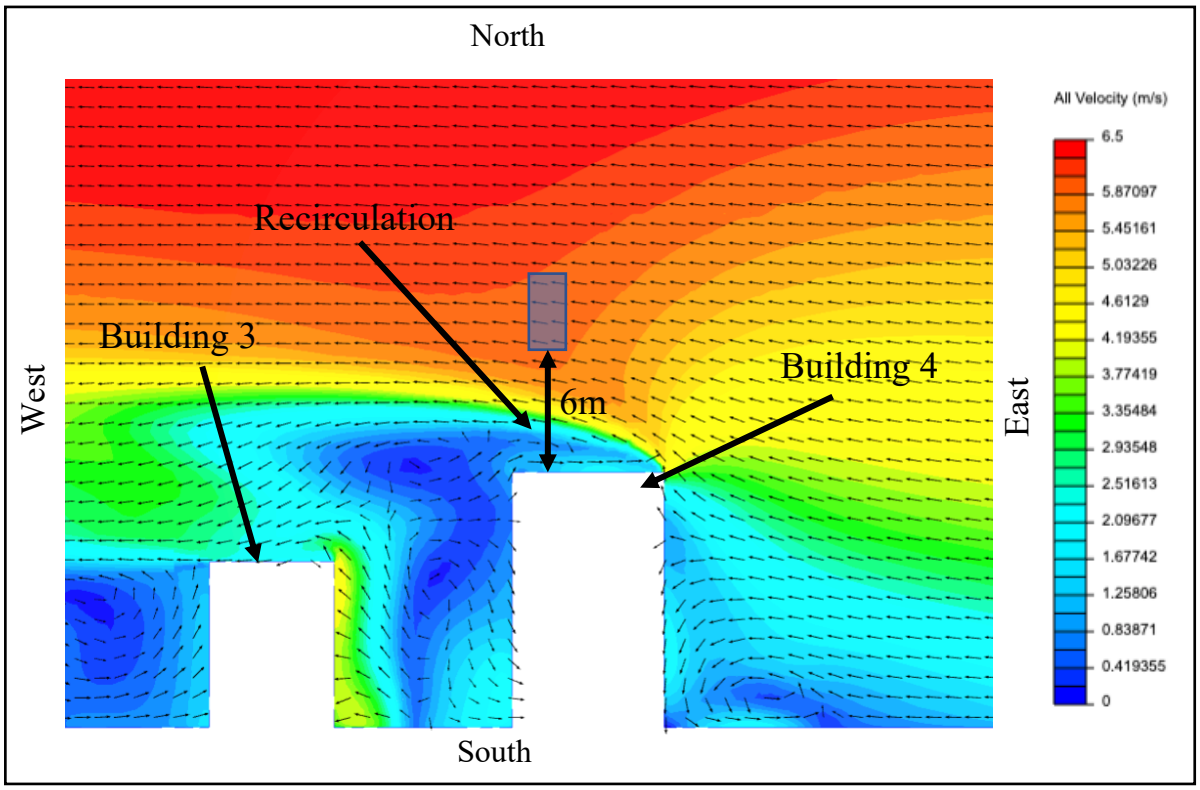

Figure 18: Wind flow over buildings 4,3 with a superimposition of a turbine at the proposed location

Being able to overcome the separation line by placing turbines above the recirculating zone, where the RANS SKE model accuracy would have been low, allows to obtain accurate velocity predictions. It has to be noted that wind's direction over the roof is partly vertical. This velocity component cannot be exploited with current VAWTs but could be useful to run the CAWTs presented in Sec.2. In addition, we can start to see that flow over building 3, and hence also buildings 1,2,6 is highly decreased due to the upwind presence of building 4.

When considering wind from either west or south-west, the speed-up effect partly occurs also on buildings 1,2,3,6 but is not as enhanced as above. This is because wind flows first over a densely built area, hence generating a huge recirculation region that surrounds all other buildings, as shown in Fig.19,20. Yet, it can be seen that, placing turbines high above roofs, it

could still be possible to exploit a partial speed-up effect that might allow turbines to produce sufficient energy. It is important to notice that, even with wind coming from the western side, the highest roof wind speeds are found on the western sides of each building, making the previous recommendation still valid for these two directions.

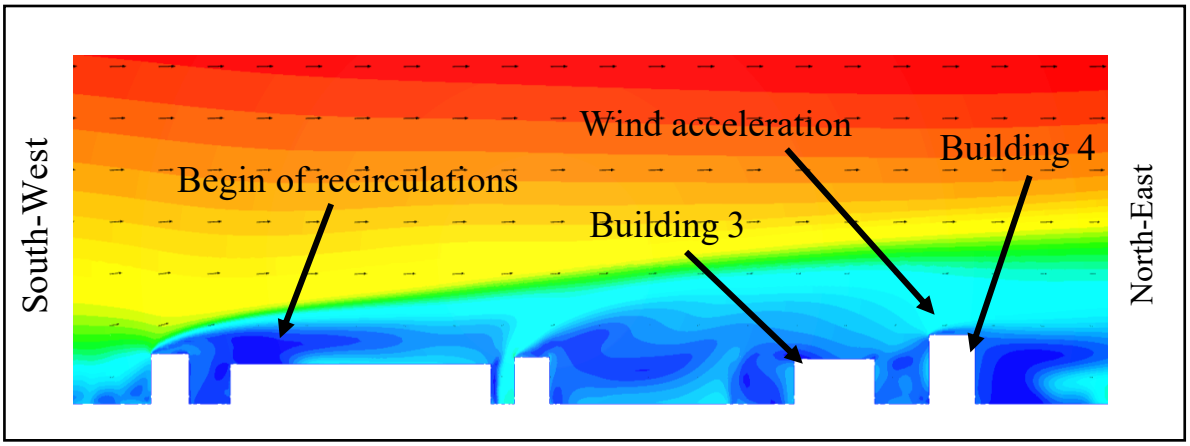

Figure 19: Simulation showing wind affecting buildings 3 and 4 when wind blows from south-west

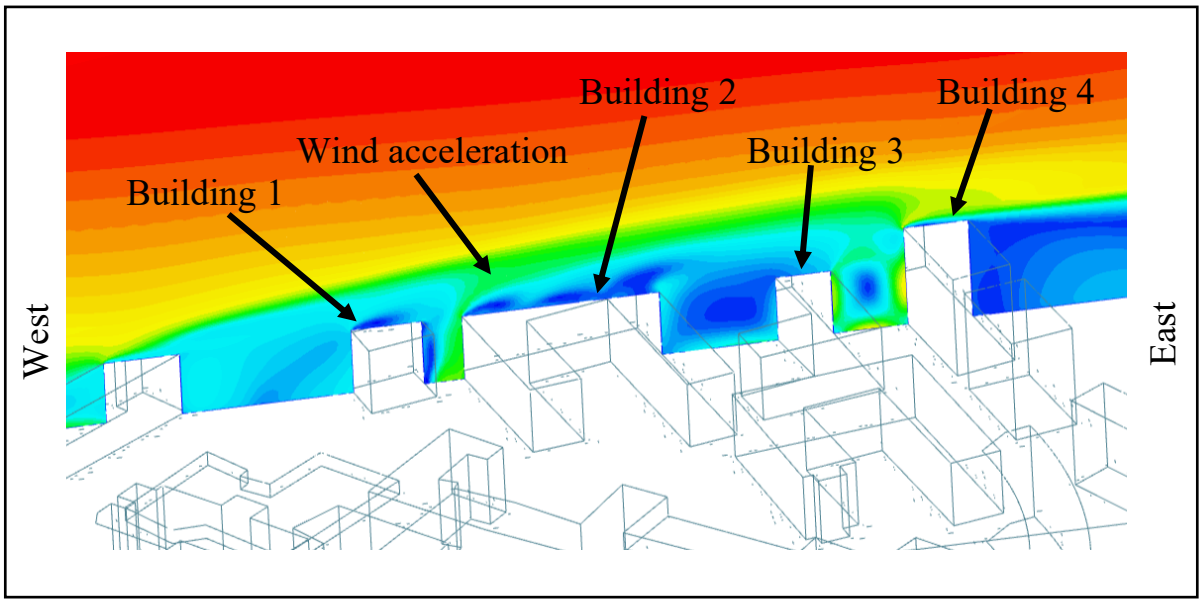

Figure 20: Simulation showing wind speeds affecting the target locations when wind blows from west

Particularly low wind speeds are therefore expected on Buildings 1,2,3,6, which are almost always surrounded by other buildings. Since, at these locations, wind varies extremely when slightly changing direction, the only suggestion that could be made would be to also locate turbines on the western side to try exploit the speed-up effect shown in Fig.19,20, which is not observed when wind blows from east.

Turbulences throughout the domain were also observed and found not to be so high to prevent instalment at any specific location. Using all these suggestions and assuming turbines would completely fill the target buildings staying at least 10m apart, the 34 target points shown in Fig.21 were selected. Two points are shown above each turbine site at respectively 6 and 12m from the rooftop, to represent the limiting heights where turbine rotors would sit.

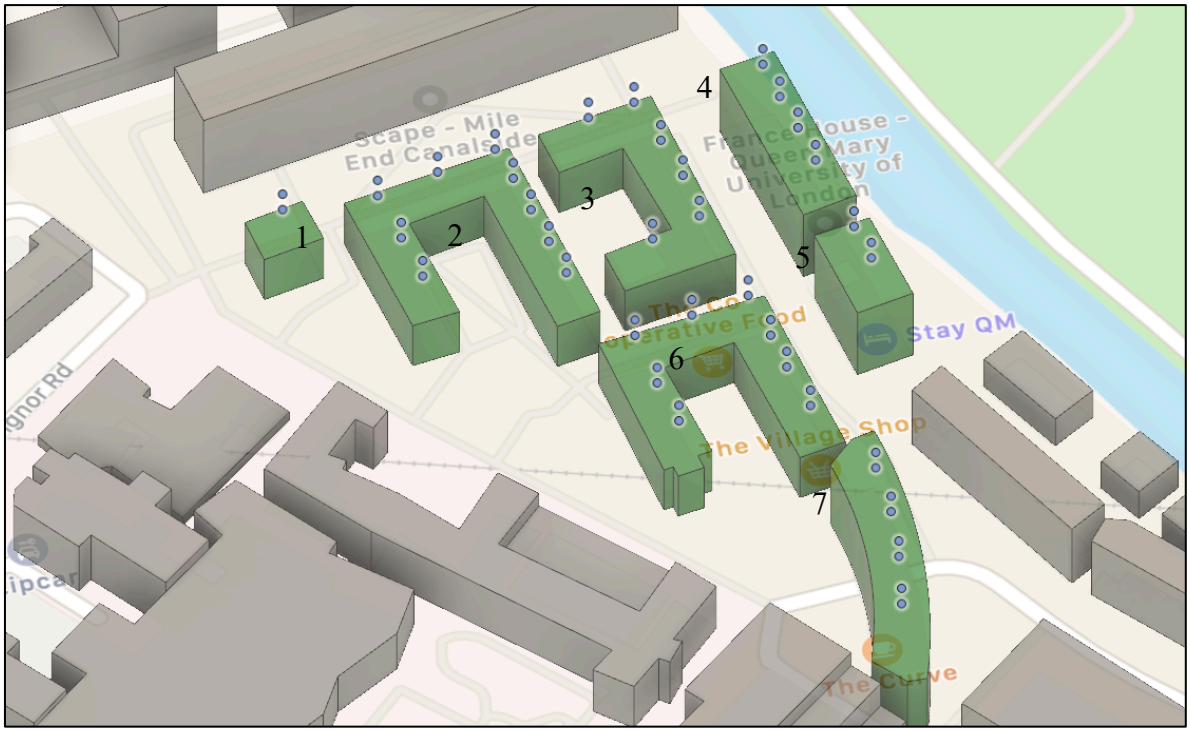

Figure 21: Representation of the selected target points for wind energy exploitation

Extracting velocities at these two points and calculating their average, it is possible to calculate how much electricity each turbine could produce, as explained in the following section.

5.3 COMPARISON OF TWO VAWTs AND THEIR ENERGY OUTPUT

The energy output of two different 10kW VAWTs having same rotor height were compared. Their key properties are all shown in Table 2 to facilitate comparison, together with the cost of 34 turbines. The first type is a Gorlov VAWT called 'Qr6', produced by Quiet Revolution and shown in Fig.22. It has been specifically created for rooftops, i.e. with a low noise, beautiful design and low weights, which can be distributed over its 3x3m base shown in Fig.23

Table 2:Major characteristic of the two vertical axis wind turbines compared in this study[25][24]

	Qr6 Gorlov VAWT	Aeolos-V 10kW H-Blade VAWT
Rotor Dimension (m^2)	6 x 3	6 x 5.5
Tower height (m)	6	7.5
Hub height (m)	9	9
Weight (kg)	1650	1730
Cut-in speed (m/s)	1.5	2.5
Cut-out speed (m/s)	20	20
Noise limit (dB)	40	43
Expected lifetime	30 years	20 years
Average price per turbine (purchasing 10+ turbines)	£44,000	£28,000
Total initial investment	£1,496,000	£952,000

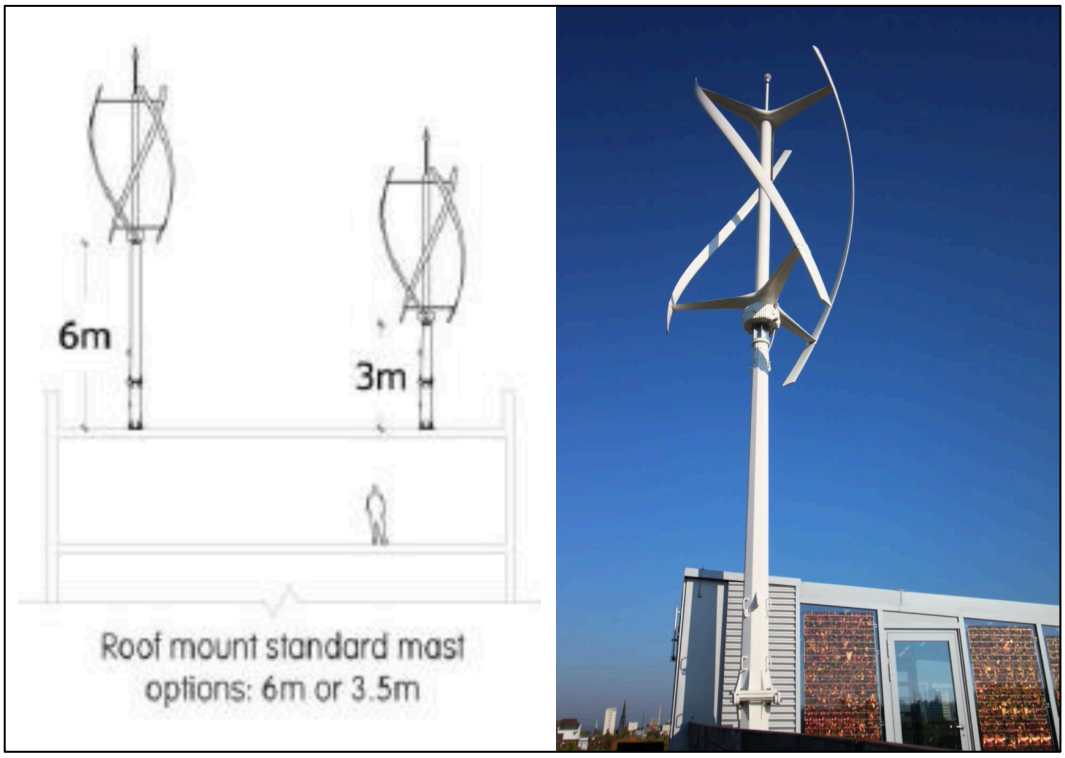

Figure 22: Schematic and real representation of the Qr6 VAWTs over roofs [24]

Figure 23: Structure supporting the tower of the Qr6 VAWT [24]

Qr6 turbine's output for each specific wind direction, i, can be calculated using Eq.3 shown in Sec.2 and the Qr6 power curve of Fig.26.

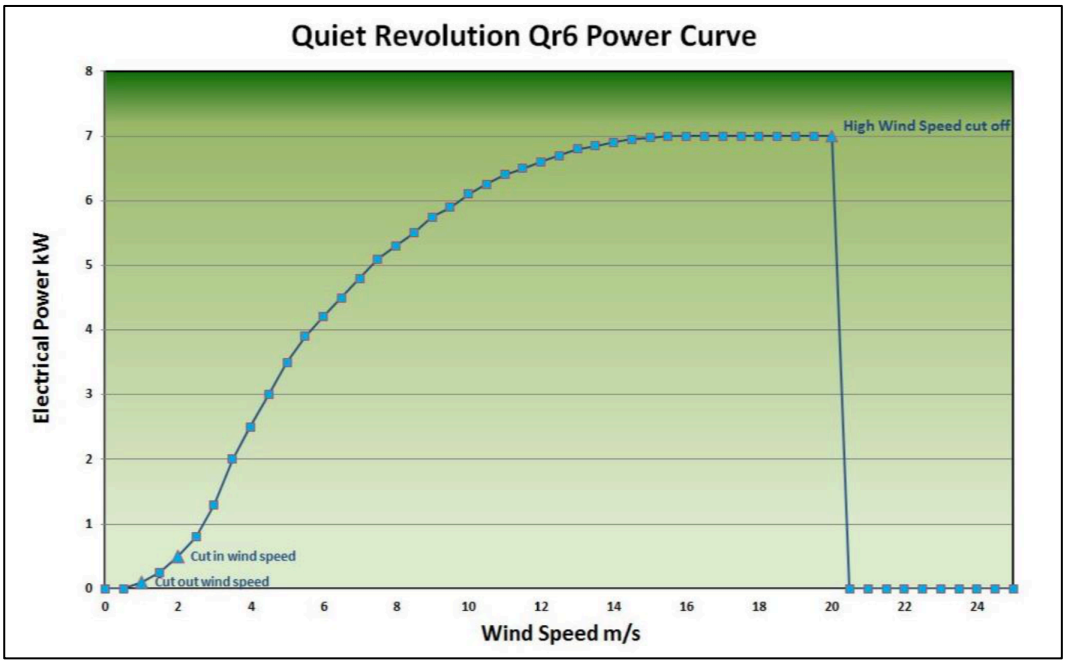

Figure 24: Qr6 Wind Turbine Power Curve [24]

The second type considered is an H-Blade VAWT, whose power output is found using the procedure explained in Sec.2.2 as its power curve is not known. The Aeolos-V 10kW turbine performance parameters are all shown in Table3.

Table 3: Aeolos-V 10kW VAWT performance parameters [25]

aerodynamic efficiency (C_p)	generator efficiency (C_g)	mechanical efficiency (C_m)	wake loss (C_w)
35%	90%,	99%	90%

Figure 25: Aeolos-V 10kW VAWT [25]

This turbine is slightly noisier and heavier, but it's cheaper, has a much higher swept area and can be placed on a base similar to the one shown in Fig.23. Its design can be seen in Fig.25

Its electricity output from each wind direction is calculated using Eq.11, assuming Rayleigh distribution around the average wind speed $\bar{u}$, obtained from the finest simulations:

$$E_{out} = (6/\pi) \cdot 0.5 \cdot \rho \cdot A \cdot \bar{u}^3 \cdot C_p \cdot C_m \cdot C_g \cdot C_w \cdot (t_i)$$

Given the different advantages and disadvantages of the two turbines, the total power outputs were compared. In both cases, the velocity used for calculations is the average ($\bar{u}$) between the highest and lowest points of each potential site, shown in Fig.21. Wind distribution of the wind rose is still accounted by assuming that yearly wind direction is proportionally spread over the

three ones analysed. Thus, wind is assumed to blow from south-west for $3{,}881 hours$, from W for $3{,}352 hours$ and from E for $1{,}527 hours$.

Assuming the installation of all 34 turbines, the total electricity produced by the whole system was calculated, together with the percentage of current consumptions that could be sustainably produced, as shown in Table 4. Assuming an electricity price of 0.15£/kWh, annual savings and the payback period of the project were also calculated.

Table 4: Key findings on the performance of the two VAWTs implemented in Queen Mary University

Number turbines	Electricity (kWh)		Percentage (%)		Annual savings (£)		Payback Period (years)	
34	Qr6	Aeolos	Qr6	Aeolos	Qr6	Aeolos	Qr6	Aeolos
	670,130	223,794	38%	15%	£100,519	£33,569	14.88	28.36

It is clear that the best design is the less noisy and more beautiful Qr6 Turbine, which allows to produce 670,130 kWh of electricity every year, i.e. 38% of current accommodations consumptions, corresponding to 190 tonnes of CO_2. Even though, as shown in Table 2, its initial investment is very high, it would be paid back in just 15 years, after which £100,519 are continuously saved for at least 5 years. In addition, it would allow saving £2,880 every year due to the Climate Change Levy Tax. Qr6's beautiful look would also allow it to obtain planning permissions more easily, especially on Buildings 4,5 in conservation areas.

The Aeolos turbine has a lower output and is almost unprofitable to run, unless its lifetime is extended beyond the expected value. Yet, it could be ideal if the University cannot undertake the £1,496,000 investment required for Qr6 turbines, while still reducing consumptions and costs by 223,794kWh and £33,569 every year.

Even though Buildings 1,2,3,6, affected by slow winds, have been considered, the overall project using either of the two turbines is extremely competitive compared to the University's solar panels, which produce only 30,000kWh. To decrease the University's initial investment, buildings 1,2,3,6 could be discarded from the project. As shown in Sec.4 in the Appendix, their production is very low, however, their implementation would still make the project profitable while cutting up to 38% emissions using Qr6 turbines.

Modelling errors and the assumption of Rayleigh distribution are present in these calculations, especially for buildings 1,2,3,6, which are always in turbulent regions. However, results in Table4 are encouraging enough to confirm the feasibility of this project up to now.

6. CONCLUSIONS

This report presents the results of a feasibility study aimed at investigating the implementation of building-mounted wind turbines (BMWTs) within Queen Mary University's campus. The most suitable locations for housing wind turbines were found to be the University's accommodations. None of them has legal planning restrictions and they all have flat roofs, high electricity consumptions and no supply from renewable sources. Furthermore, their consumptions were found to have the same daily trends of wind speed, suggesting that batteries for electricity storage could not be necessary.

Using CFD to simulate wind flow over the University's accommodations, two recurrent effects were noticed. The first buildings hit by the wind always show a speed-up effect on their roofs, which is more intense on the downwind side of the building. Furthermore, when wind flows over a block of houses, a tall recirculation region of decreased wind speeds develops and incorporates most buildings located downwind. This creates particularly low wind speeds for buildings 1,2,3,6, which have lower roofs than surrounding constructions. These two effects combined generate different patterns for almost any wind direction tested. Based on the three simulations conducted here, the major suggestion for enhancing wind power utilisation is to place turbines on the western side of all buildings. This would allow to harvest the local speed-up effects over most roofs.

The potential electricity output at the proposed locations was calculated for two different turbines to conclude that it would be feasible for the University to substantially decrease its buildings' costs and emissions using BMWTs. The recommended turbine is the less noisy, more beautiful and productive Qr6 VAWT. Implementing 34 turbines, up to 38% of all target buildings' current consumptions could be produced. Even though an initial investment of £1,496,000 is required for Qr6 turbines, after only 15 years the project would become profitable, allowing an extra saving of £100,519 for at least 5 other years.

Carrying on from this, the University should analyse wind flows using LES turbulence model, considering all wind directions and physically measuring wind speeds. Target locations should be structurally assessed to ensure that safe turbine installation can be ensured, and a more formal proposal should be presented to Tower Hamlets to obtain planning permissions.

This positive outcome of this project alone is, however, not enough to categorically confirm the feasibility and profitability of BMWTs in all urban environments. Future works in this field should focus on assessing the wind resource of other urban sites and developing specifically designed wind turbines for these areas. Continuous improvements of innovative turbines such as cross-axis wind turbines (CAWTs), for example, will be invaluable to spread awareness on and make the best of this yet unexploited sustainable resource. This could then lead to high reductions of both electricity costs and CO_2 emissions in urban locations, an invaluable target for the future of our cities.

STUDENT'S AND OTHERS' CONTRIBUTION TO PROJECT:

This project was completed with the support of both Queen Mary University Staff and external companies. I would like to personally acknowledge Dr Philip Tamuno, Queen Mary (QM) Head of Sustainability, Luciana Pennaroli, QM Space Data Manager, and Timothy Lee, QM CEng Technical Manager (Infrastructure and Maintenance), for guiding me through the project and providing all necessary raw data on Queen Mary's electricity consumptions. The kind contribution of Meteoblue.com, who provided wind raw data, has also been of noticeable importance. I would also like to point out the generous availability of Chris Newland, Managing Director at Global Partnerships Limited, and Alicia Wang of Lotus Energy Technology who kindly provided all data regarding their wind turbines. All CFD simulations have been successfully completed thanks to SimScale staff, who provided the necessary amount of core hours to complete my simulations as well as guidance on how to use their software. The assistance of all these people and institutions has been crucial to successfully complete this project. I would like to finally remark that all results that have not been specifically referenced in this report have been obtained exclusively by me or by processing provided raw data.

ACKNOWLEDGMENTS:

I would like to express my deep sense of gratitude and respect to my project supervisor, Dr. Adrian Briggs, who constantly provided the guidance, support and recommendations that helped me achieve the completion of this project. His constant supervision allowed me to grow under both personal and professional aspects. I should also express my appreciation for the support provided by Dr. Jens-Dominik Mueller, who provided the necessary assistance to complete my project simulations.

REFERENCES:

[1] IEA.org, "World Energy Outlook 2019," *IEA, Paris*, 2019. https://www.iea.org/reports/world-energy-outlook-2019 (accessed Mar. 24, 2020).

[2] Great Britain - Climate Change Act, "Elizabeth II, The Stationary Office," London, 2008 (Chapter 27), 2008.

[3] A. S. Yang, Y. M. Su, C. Y. Wen, Y. H. Juan, W. S. Wang, and C. H. Cheng, "Estimation of wind power generation in dense urban area," *Appl. Energy*, vol. 171, pp. 213–230, Jun. 2016, doi: 10.1016/j.apenergy.2016.03.007.

[4] S. L. Walker, "Building mounted wind turbines and their suitability for the urban scale-A review of methods of estimating urban wind resource," Elsevier B.V., 2011.

[5] A. G. Dutton, J. Halliday, and M. J. Blanch, "The Feasibility of Building-Mounted / Integrated Wind Turbines (BUWTs): Achieving their potential for carbon emission reductions," London, 2005.

[6] M. Casini, "Small Vertical Axis Wind Turbines for Energy Efficiency of Buildings," *J. Clean Energy Technol.*, vol. 4, no. 1, pp. 56–65, 2015, doi: 10.7763/jocet.2016.v4.254.

[7] Y. Li, "Straight-Bladed Vertical Axis Wind Turbines: History, Performance, and Applications," *Rotating Mach.*, pp. 1–17, 2020.

[8] V. Upadhyaya, "Technical and Financial Feasibility for Small Scale Wind Turbines in Urban Areas of Jaipur," vol. V, no. Ii, pp. 8–17, 2016.

[9] W. T. Chong, M. Gwani, C. J. Tan, W. K. Muzammil, S. C. Poh, and K. H. Wong, "Design and testing of a novel building integrated cross axiswind turbine," *Appl. Sci.*, vol. 7, no. 3, 2017.

[10] T. Pelucchi, "Project Rationale, Aims and Objectives," no. November, pp. 1–11, 2019.

[11] F. Toja-Silva, T. Kono, C. Peralta, O. Lopez-Garcia, and J. Chen, "A review of computational fluid dynamics (CFD) simulations of the wind flow around buildings for urban wind energy exploitation," *J. Wind Eng. Ind. Aerodyn.*, vol. 180, pp. 66–87, 2018.

[12] J. T. Millward-Hopkins, A. S. Tomlin, L. Ma, D. B. Ingham, and M. Pourkashanian, "Mapping the wind resource over UK cities," *Renew. Energy*, vol. 55, pp. 202–211, Jul. 2013.

[13] J.-D. Müller, *Essentials of computational fluid dynamics*, 2015/10/13. London, UK: CRC Press, 2016.

[14] L. Lu and K. Y. Ip, "Investigation on the feasibility and enhancement methods of wind power utilization in high-rise buildings of Hong Kong," Hong Kong, 2009.

[15] D. Micallef and G. Van Bussel, "A review of urban wind energy research: Aerodynamics and other challenges," *Energies*, vol. 11, no. 9, pp. 1–27, 2018.

[16] M. A. Heath, J. D. Walshe, and S. J. Watson, "Estimating the potential yield of small building-mounted wind turbines," *Wind Energy*, vol. 10, no. 3, pp. 271–287, 2007.

[17] M. H. Ouahabi, F. Benabdelouahab, and A. Khamlichi, "Analyzing wind speed data and wind power density of Tetouan city in Morocco by adjustment to Weibull and Rayleigh distribution functions," *Wind Eng.*, vol. 41, no. 3, pp. 174–184, 2017.

[18] QM University, “Queen Mary University of London - Sustainability,” 2020. http://www.estates.qmul.ac.uk/about/sustainability/ (accessed Mar. 06, 2020).

[19] Meteoblue, “Weather History+ dataset,” 2020. https://www.meteoblue.com/it/historyplus (accessed Jan. 02, 2020).

[20] S. Emeis, *Wind energy meteorology : atmospheric physics for wind power generation*. New York: Springer, 2013.

[21] Chris Blandford Associates, “Tower Hamlets Conservation Strategy 2026,” London, UK, 2017.

[22] Architectural Institute of Japan (AIJ), “Benchmarks for Validation of CFD Simulations Applied to Pedestrian Wind Environment around Buildings Architectural Institute of Japan,” Tokyo, 2016.

[23] J. Franke, A. Hellsten, K. H. Schlünzen, and B. Carissimo, “The COST 732 Best Practice Guideline for CFD simulation of flows in the urban environment: A summary,” *Int. J. Environ. Pollut.*, vol. 44, no. 1–4, pp. 419–427, Feb. 2011, doi: 10.1504/IJEP.2011.038443.

[24] QuietRevolution, “QR6 Vertical Axis Wind Turbine,” 2020.

[25] Lotus Energy Technology, “Aeolos-V 10kW,” *Efikasi Diri dan Pemahaman Konsep IPA dengan Has. Belajar Ilmu Pengetah. Alam Siswa Sekol. Dasar Negeri Kota Bengkulu*, vol. 6, 2020.

[26] Tower Hamlets, “LOCAL PLAN 2031 ADOPTED POLICIES MAP,” 2020.

APPENDIX:

This section provides additional information that were invaluable to complete this report. Larger sets of raw data used in the report such as buildings consumptions and yearly wind speed variations can be provided upon request to any user willing to analyse them.

1. WIND RAW DATA OBTAINED FROM METEOBLUE.COM

Table 5: Quantitative representation of the wind rose provided by Meteoblue.com for Queen Mary University of London's site.

Location: 51.53°N 0.04°W							
Period: 11/03/19 – 11/03/20							
Variable: Wind Speed							
Unit: occurrences							
Height: 10 m							
Wind Speed (m/s)	1	3	5	7	9	11	13
N	247	345	104	5	0	0	0
NE	275	219	87	1	0	0	0
E	324	452	163	0	0	0	0
SE	235	394	57	1	0	0	0
S	255	267	132	24	0	0	0
SW	383	907	732	282	65	15	2
W	360	761	687	231	21	0	0
NW	210	397	123	36	8	1	0
TOTAL	2289	3742	2085	580	94	16	2

2. TARGET LOCATIONS SELECTED AT QUEEN MARY UNIVERSITY

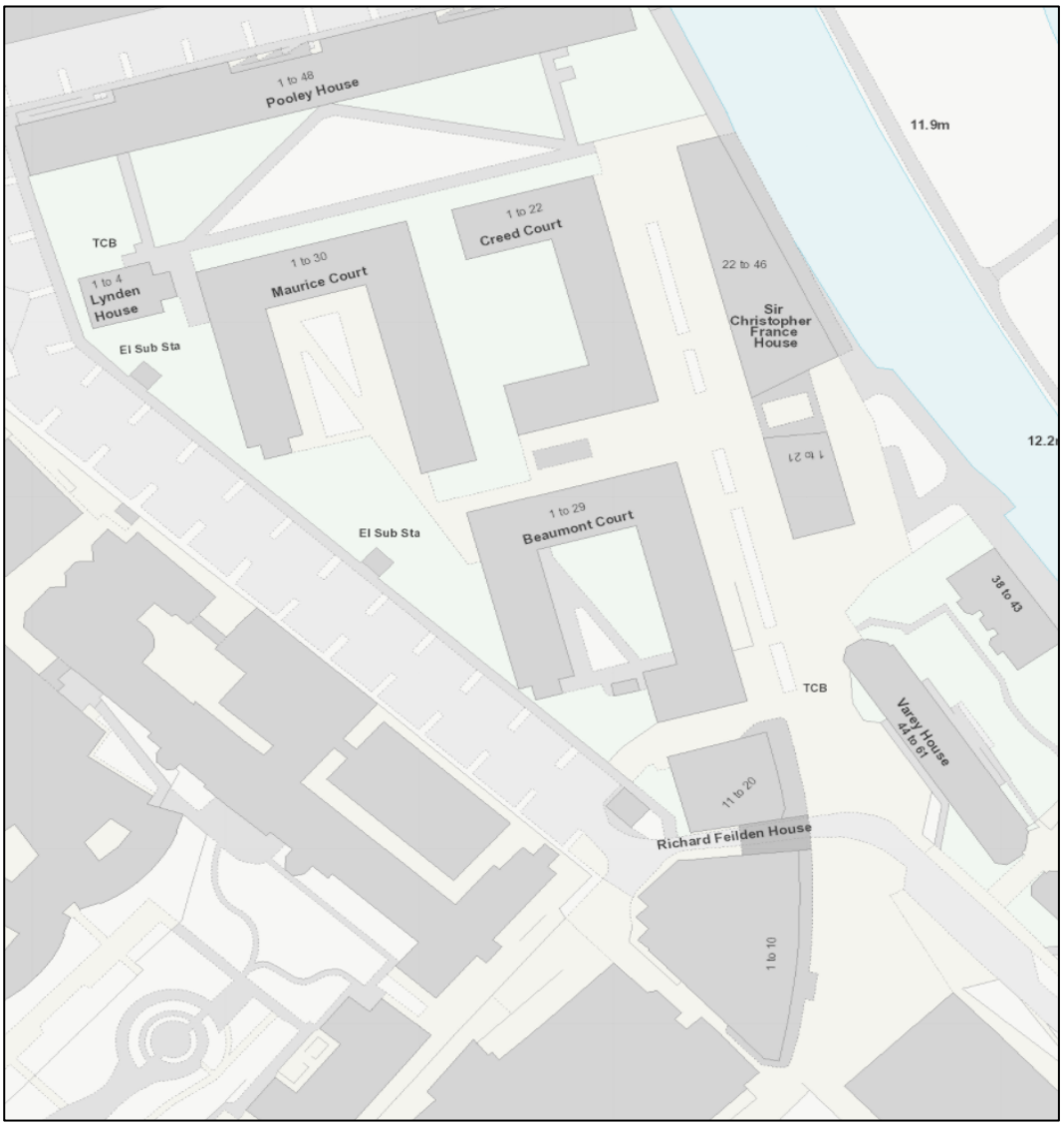

Figure 26: Detailed image of the target locations selected at Queen Mary University of London [26]

3. DETAILED EXPLANATION OF THE VALIDATION BENCHMARK CASE STUDY

Since the aim of the project is to simulate flow over multiple buildings of Queen Mary University, the benchmark case study shown below, conducted by the Architectural Institute of Japan (AIJ), would be the most suitable. It considers flow over scaled-down cuboid buildings with side length D=0.2m (AIJ, 2016). Having tested the model in a wind tunnel using a probe to measure velocities, as shown in Fig. (a), the AIJ provides actual velocity measurements at all points shown in Fig. (b).

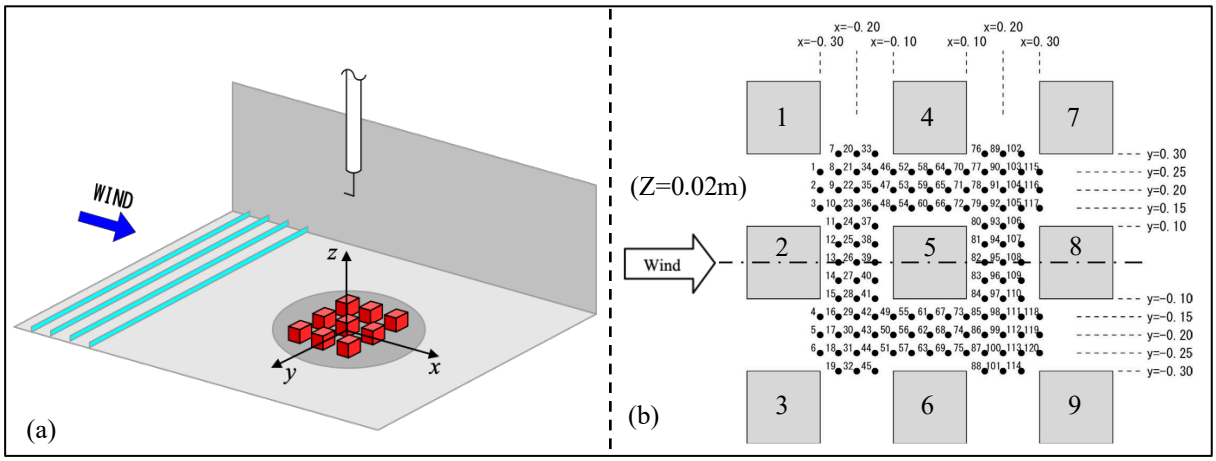

Figure 27: Experimental procedure used by the AIJ (a) used to evaluate velocities at all red points (b) (AIJ, 2016)

3.1 SETTING UP THE SIMULATION

Such a geometry is first modelled in CAD using Fusion 360 and then imported in SimScale. The parameters that have to be validated using this case include mesh layout, turbulence model, boundary conditions (BCs), initial condition and assumptions of constant density and viscosity. This would then allow to understand the discrepancies between the simulation and reality. The computational domain suggested by the AIJ has the same dimensions of the wind tunnel used for testing, i.e. 3m wide, 3m long and 1.8m high, with the building array positioned in the middle, as shown below.

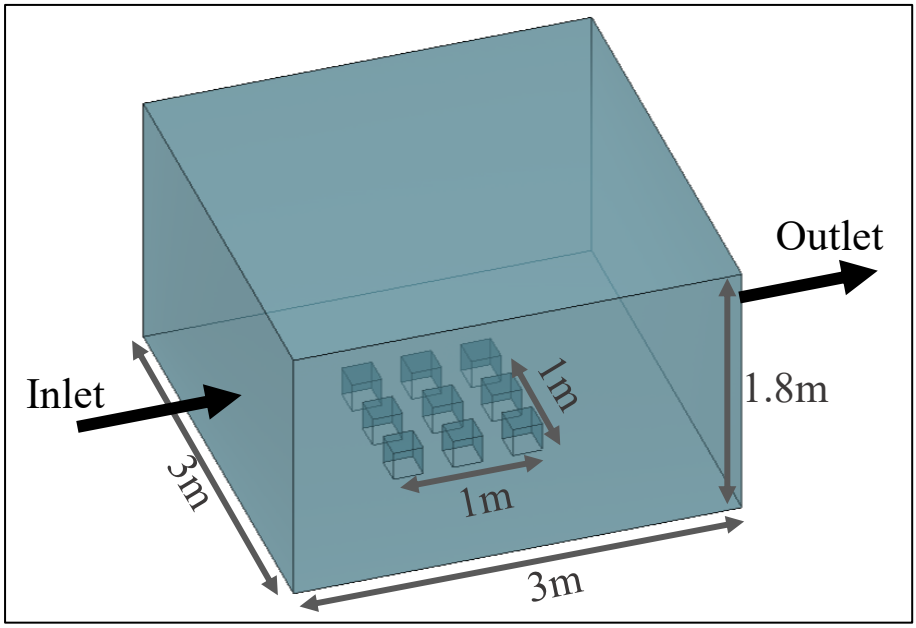

Figure 28: Dimensions of the computational domain used for validation

As suggested by the AIJ (2016), the inflow wind profile can be well approximated using the power law, shown in Eq. 1, where, for this case, α = friction coefficient = 0.28.

$$u(z) = u(z_r)\left(\frac{z}{z_r}\right)^{\alpha} \text{ [20]}$$

z = height from ground, $u(z)$ = x velocity at height z, z_r = reference height.

Plotting the velocity wind profile, taking $z_r = 0.15m$ and $u(z_r) = 3.483m/s$, the inlet boundary to be validated is:

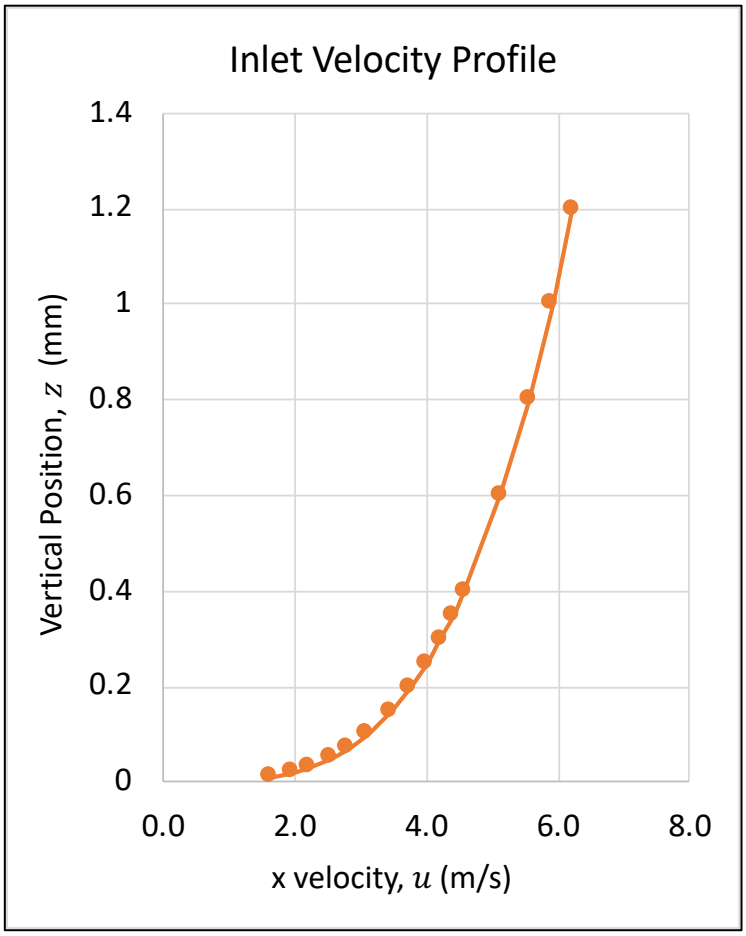

Figure 29: Inlet velocity profile used for the validation case

At the outlet, the velocity magnitude is not specified, in order to allow the flow to modify freely, depending on what happens in the domain. Therefore, gauge pressure at outlet is set as 0 Pa. All remaining BCs, i.e. buildings walls, the terrain and sides of the wind tunnel, are set as Wall No-Slip boundary condition, meaning that velocity there is zero. The flow used in these simulations is considered to be air with a fixed density and viscosity of respectively 1.1965 kg/m^3 and 1.529 m^2/s. In addition, as mentioned in Sec.2 and suggested by the AIJ,

the steady RANS SKE turbulence model is exploited to look for the steady state solution. Finally, the initial condition of the flow was set as $u_x = 3\ m/s$.

3.2 IDENTIFICATION OF THE BEST MESH LAYOUT

In order to properly run simulations and avoid excessive errors, it is crucial to create a suitable, tailored mesh for each simulation. The mesh has to be small enough to reduce the effects of artificial viscosity (AV), which acts like a physical viscosity but is purely caused by the numerical discretisation of the simulation [13]. AV is directly proportional to the gradients in flow quantities, hence, is high in regions of high changes, such as corners or stagnation points, where a finer mesh is required. To decrease AV, simulations here are also run using a second order accuracy, which is the highest available for SimScale users. Major factors to be taken into account when generating the mesh are its skewness (angles within mesh shouldn't be greater than 120°), regularity (opposite sides of cells should be as parallel as possible) and smoothness (variations of elements size should occur gradually) [13]. Refining the mesh only where required and keeping a coarser mesh in regions of low variations also allows to maintain computational times relatively low, while achieving more accurate results.

Having considered all these guidelines, a structured mesh with quadrilateral elements has been chosen. To begin understanding the flow, an initial simulation is run with a very coarse mesh and no specific refinements. Having understood the general patterns of the flow, several meshes are created and run to compare their results. As proven by this first simulation, the highest flow

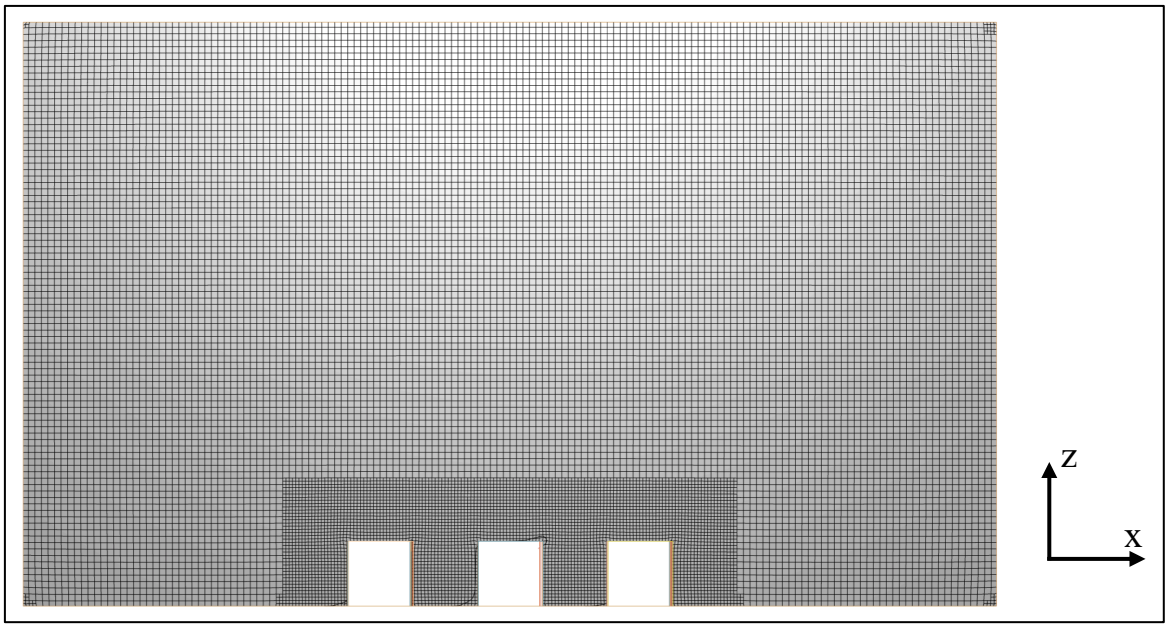

Figure 30: Cross section of the domain showing grid discretisation after first refinement

variations are observed within the 9 buildings. Therefore, a refinement was created within a rectangular region, as shown in the figure above.

Cross section of the domain showing grid discretisation after first refinement Even though after this improvement started to match wind tunnel measurements more closely, the average error was still around 38.2%. Therefore, a few corrections were made to the mesh. Since the transition from coarse to finer elements happens suddenly in the figure above, a smoother transition was introduced. In addition, a series of very small boundary layer elements were introduced against the lowest side of the domain ($z = 0$). In fact, as shown by the inflow profiles, flow properties can vary noticeably in this bottom region. In addition, since the 9 shapes have all sharp corners, flow variations are also common on their surfaces. Hence, a surface refinement was implemented on all buildings' surfaces. After this improvement, the mesh generated can be seen in the figure below, which has an average discrepancy with wind tunnel data of about 36%.

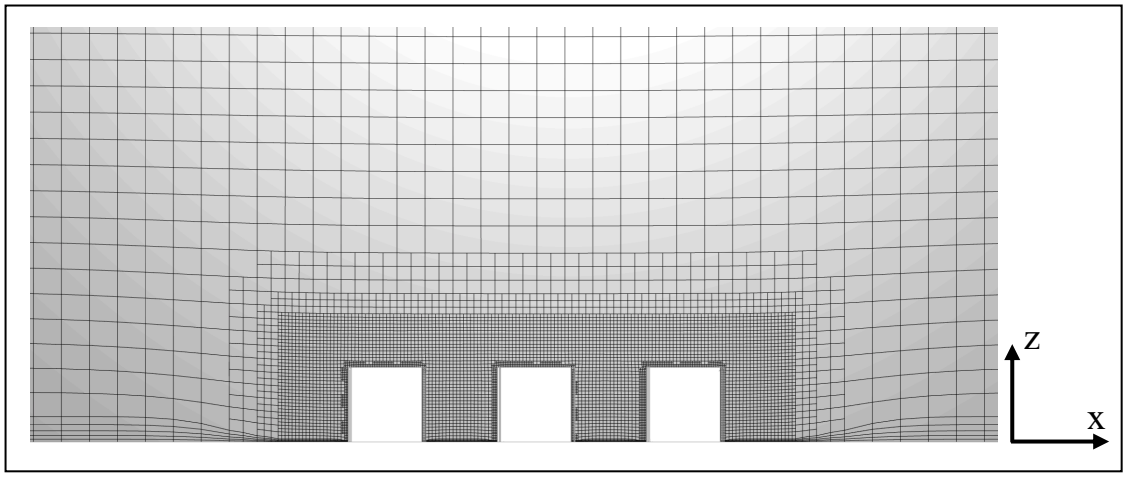

Figure 31: Zoomed in version of the second refinements of the mesh

As we can see, the mesh becomes smoothly finer from free stream to the surface of the buildings. In addition, it is clear that the refinement of the bottom boundary layer is proportional to the overlaying mesh, hence it also becomes increasingly fine as we approach the buildings block. After trying this mesh, three additional modifications were tested. First of all, an even more refined region was created to include all buildings in the first row because it is here that the highest changes are observed, due to wind impinging against the front surface of the buildings and hence creating a stagnation point. Fig. shows the view from above for this refinement.

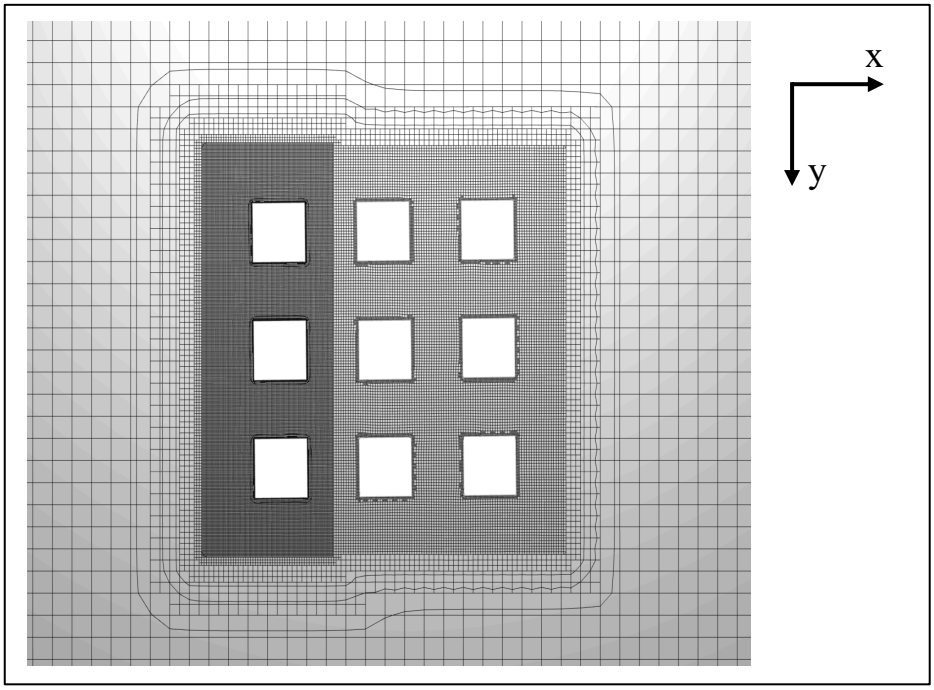

Figure 32: Top view of the third mesh refinement tried

However, this improvement was not considered as the error did not increase enough to justify the increased computational time required by the software to complete this simulation, compared to a previous one.

Finally, the computational domain was enlarged upstream and downstream, in order to allow the flow to develop respectively before and after encountering the 9 houses. An improvement was observed only when the x-distance between the inlet and the first building was increased from $1m$ to $1.5m$. This allowed to reduce the error to 34.251% while using a relatively coarse mesh. The final mesh that was eventually chosen for this case can therefore be seen in the two figures below.

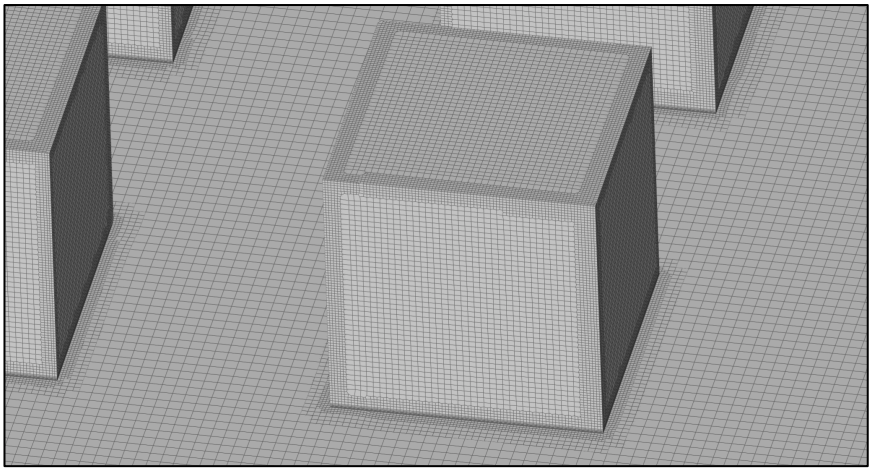

Figure 33: Detail of one cube of the final mesh used

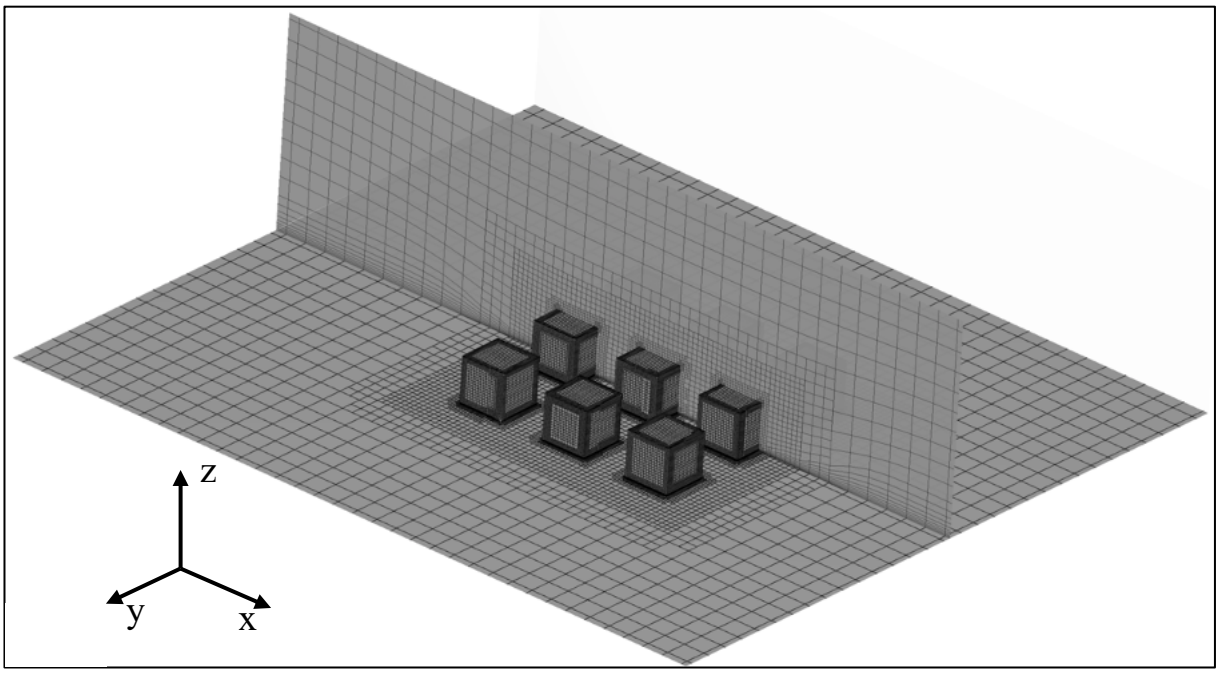

Figure 34: Final mesh used for the benchmark case study

Using this mesh parameters, three increasingly fine meshes were tested and constantly compared with wind tunnel measurements to understand if mesh convergence was eventually achieved.

3.3 BENCHMARK CASE AND EXPERIMENTAL RESULTS COMPARISON

Since the aim of all simulations is to achieve steady state, before using simulations results, it is important that each run has achieved time convergence, i.e. the solution does not change if the simulation is run for more time. To do so, the residual in each cell, i.e. the rate of change of a specific quantity, has to tend towards zero. SimScale automatically provides a plot of the residual of the three velocity components (u_x, u_y, u_z) and the TKE. The graph below shows a typical convergence plot where the residuals tend continuously towards zero. However, these values represent the RMS (Root Mean Square) taken over all cells. Therefore, even though it tends towards zero, there might still be some cells where quantities are changing noticeably.

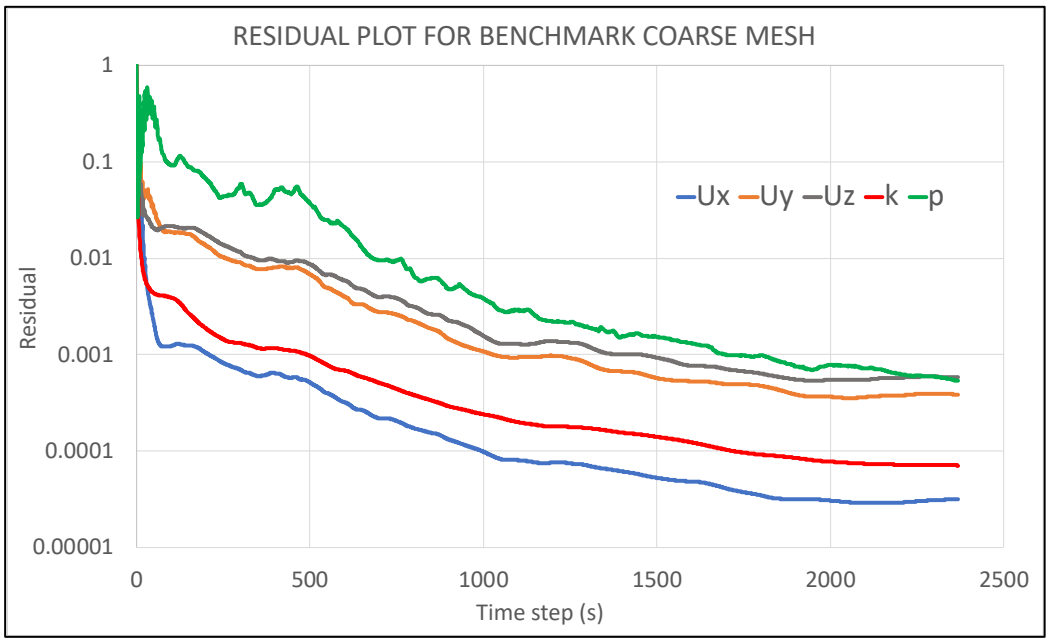

Figure 35: Typical residual plot of the benchmark case study

The x-velocities are therefore measured as they are the major focus of this study. Time variation of this quantity was monitored at several points within the domain, especially in proximity of the nine blocks. The results obtained for four different points of the finest simulation can be clearly seen below:

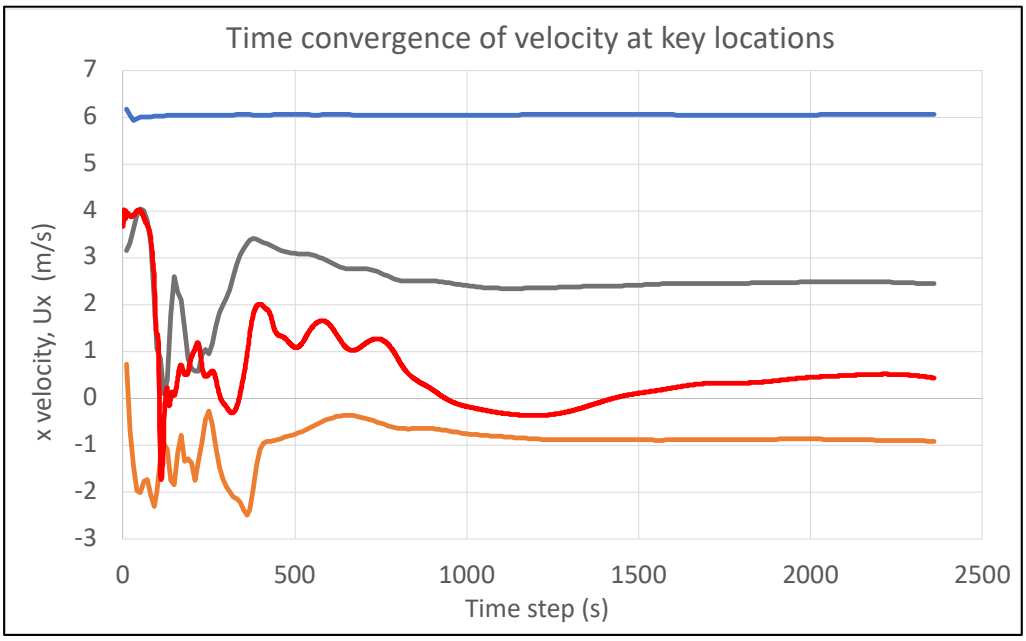

Figure 36: Monitoring of x velocities variations in time

This graph shows that velocity at all these key points of the domain converged in time. The only point that shows still some variations at the end of the simulation is that plotted in red. However, this point was placed in a highly turbulent region and its changes are so small to be

considered acceptable. This procedure was followed for all simulations, making sure that time convergence was always achieved.

Subsequently, the results of three increasingly fine meshes were analysed. In particular, velocity ratios at all points shown at the beginning of Sec.2 were extracted from each mesh and compared with experimental data. Velocity ratios are values normalised with the velocity at inlet. Table 1 shows the overall average error that was obtained for each mesh

Table 6: Comparison of errors obtained from three increasingly fine meshes

	Coarse Mesh	Medium Mesh	Fine Mesh
Number of mesh elements	$305 \cdot 10^3$	$1.7 \cdot 10^6$	$10.8 \cdot 10^6$
Percentage overall error with experimental data	30.244 %	30.480 %	30.099 %

In order to better understand these errors, the velocity magnitude at each point was compared with real measurements using graphs, however, since these points would be too many for only one plot, the high-turbulent regions were plotted in a different graph. To do so, the Surface LIC feature of the post-processing software Paraview shown below was used.

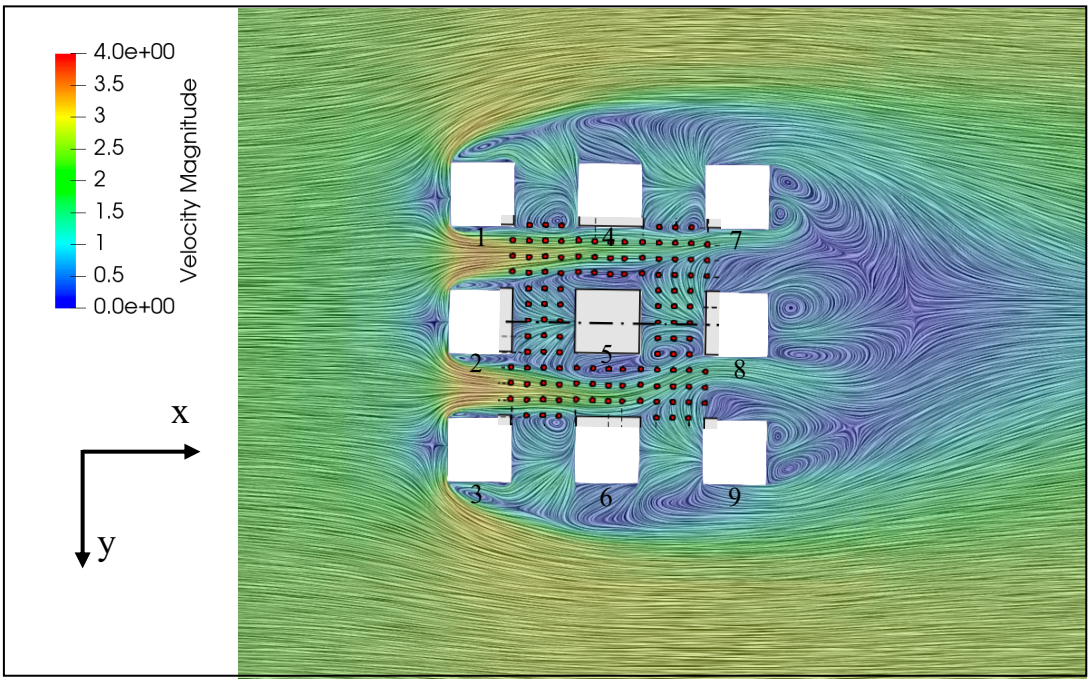

Figure 37: Surface LIC view of the finest mesh at z=0.02m with superimposition of probe points

The Surface LIC feature clearly allows to understand the flow pattern at every point, while seeing the velocity magnitude. First of all, we can see an increase in velocity as soon as the flow starts flowing in between buildings, similar to the Ventui effect presented in Sec. 2. Subsequently, various turbulences develop. The probe points where the flow is most turbulent are located behind buildings 1 and 3 as well as all around building 5. By plotting velocity ratios at these points for all three meshes tested, it is possible to compare them with the experimental data. On the x-axis, the following graph plots the number of each point:

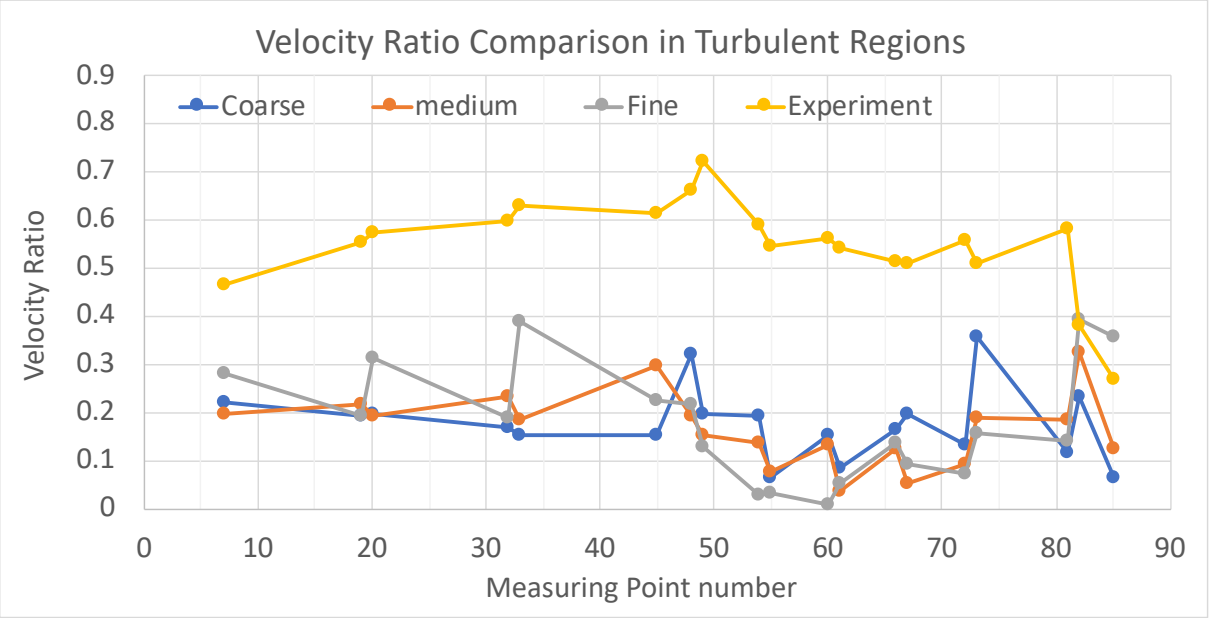

Figure 38: Comparison of simulation and experimental results in turbulent regions of the benchmark study at z=0.02m

In this case, we can see that there is a noticeable difference between the simulation and experimental values. In addition, when refining the mesh, two different paths are observed. For points numbered from 0 to 45, i.e. points behind buildings 1 and 3, refining the mesh gives values closer to the experiment, however, an inverse pattern is observed for all remaining values, which represent points surrounding building 5. This phenomenon could be due to the increased turbulences not being improved when refining the mesh. However, if we consider all the other measurement points, a closer match with the experiment is obtained. The following graph only shows data for some points in laminar flow, in order to better visualise their patterns.

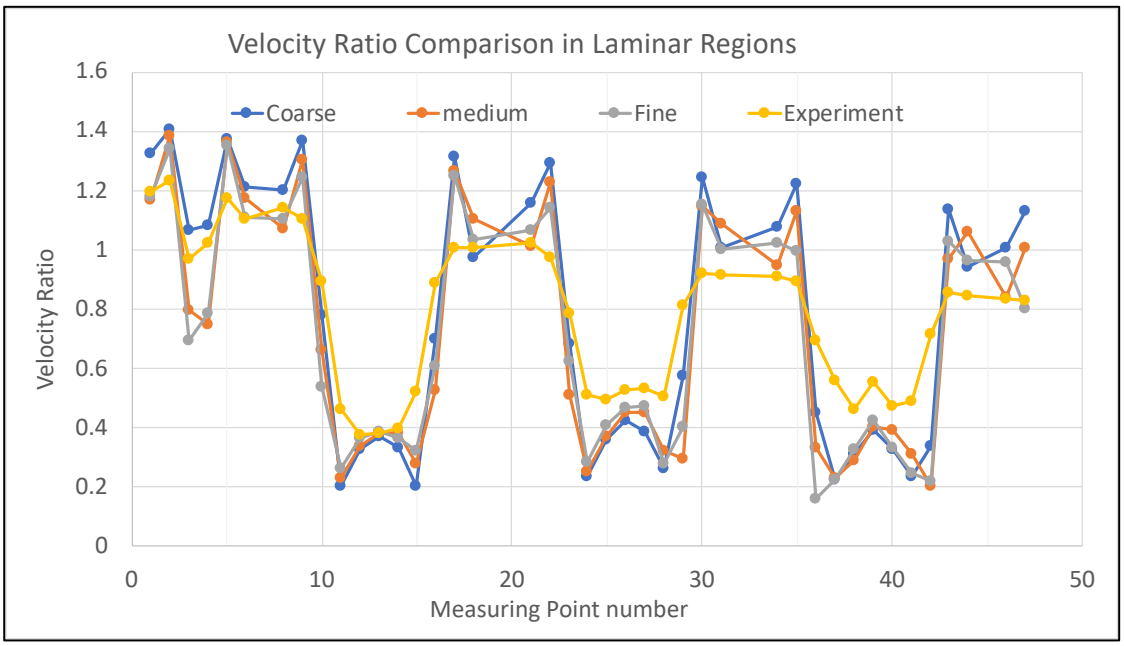

Figure 39: Velocity ratio at points in laminar region, compared with experimental data

This graph clearly shows that, overall, as the mesh is refined, values tend towards those provided by the AIJ. This is especially evident at data points between 10 and 15. However, it is still not possible to state that mesh convergence has been achieved in all regions. In fact, there are still discrepancies with the measured data and the finest simulation. Yet, the discrepancy is relatively small and, most importantly, trends are extremely similar. As the computational times of the finest simulation were almost 168 core hours for the finest mesh, no further refinements were made. In addition, since the overall error is only about 30%, as shown in the table above, still accounting for high errors in turbulent regions, it is possible to say that sufficiently accurate results are achieved, and the model can be considered validated. It is still important to remember that velocity magnitudes in highly turbulent, recirculating regions are not extremely well predicted by the model.

4. ADDITIONAL INFORMATION ON QUEEN MARY UNIVERSITY'S CFD SIMULATIONS

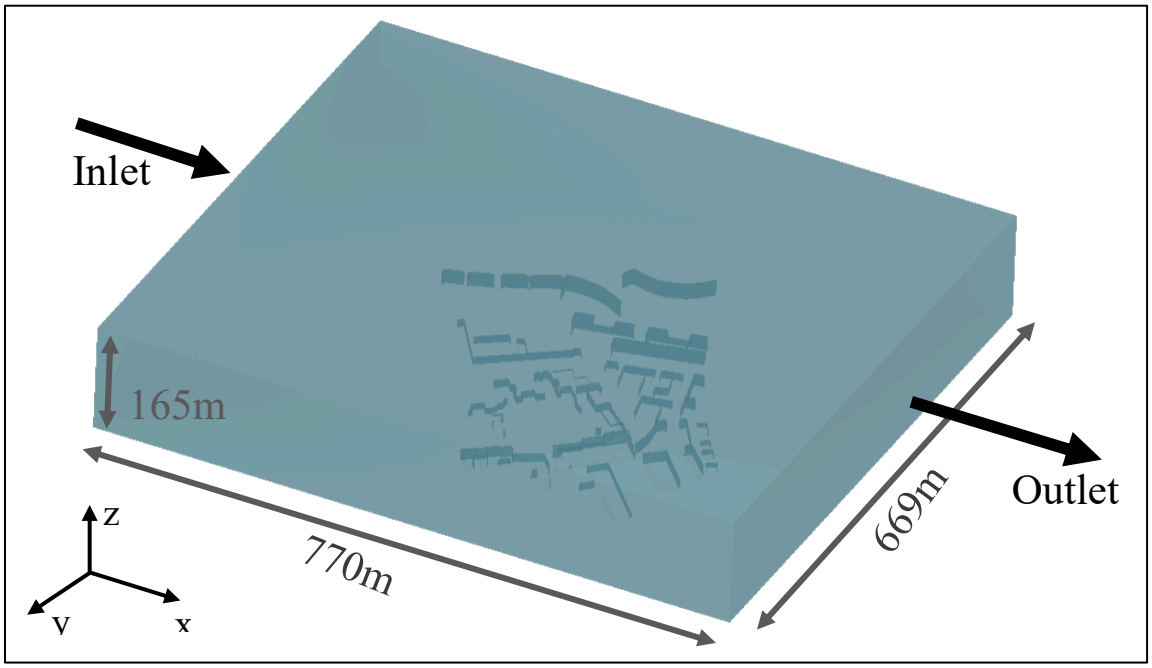

Figure 40: Dimensions of the domain used for simulations with wind blowing form west

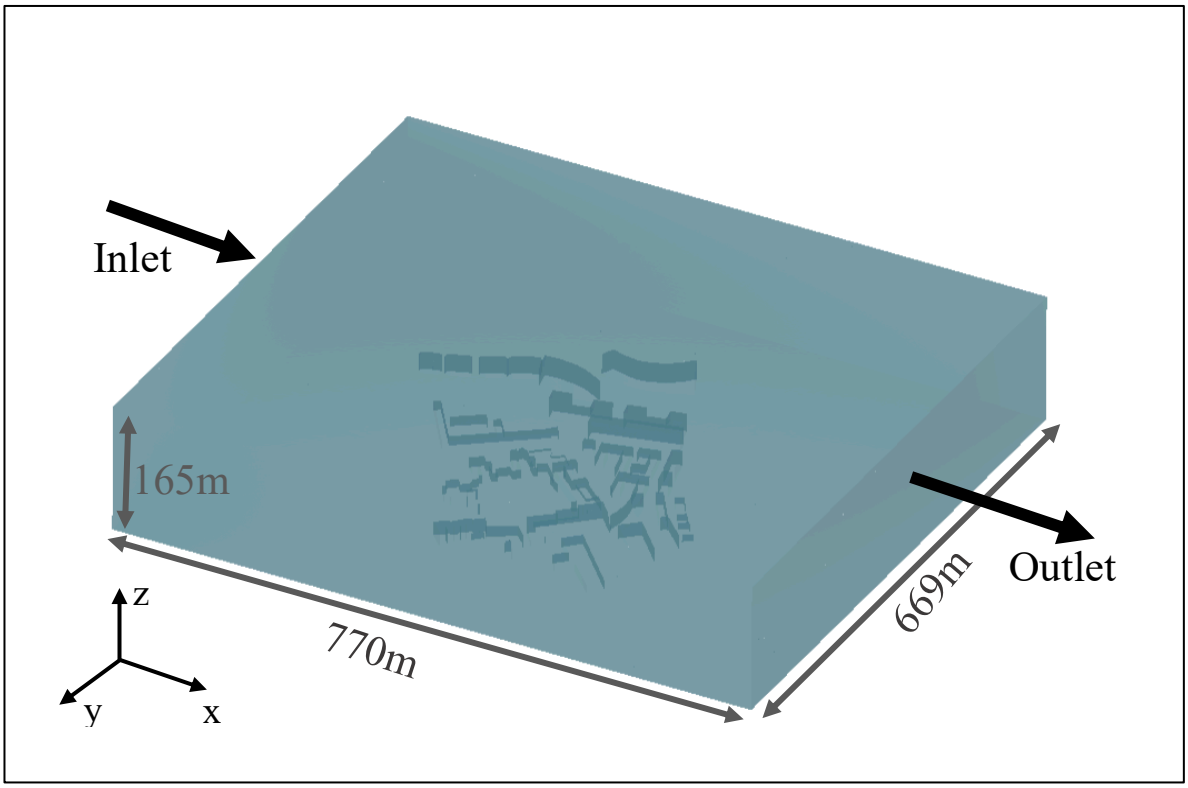

Figure 41: Dimensions of the domain used for simulations with wind blowing form east

Table 7: Size of all the meshes used to simulate wind flow over Queen Mary University

Wind Direction	Mesh type	Number of elements	Number of nodes
South West	Coarse	$9.1 \cdot 10^6$	$10.3 \cdot 10^6$
	Medium	$15.1 \cdot 10^6$	$16.7 \cdot 10^6$
	Fine	$38.5 \cdot 10^6$	$39.9 \cdot 10^6$
West	Coarse	$9.7 \cdot 10^6$	$10.8 \cdot 10^6$
	Medium	$16.1 \cdot 10^6$	$17.6 \cdot 10^6$
	Fine	$24.9 \cdot 10^6$	$26 \cdot 10^6$
East	Coarse	$9.7 \cdot 10^6$	$10.8 \cdot 10^6$
	Medium	$16.1 \cdot 10^6$	$17.6 \cdot 10^6$
	Fine	$22.4 \cdot 10^6$	$24.3 \cdot 10^6$

5. DETAILED INFORMATION ON THE TWO ANALYSED TURBINES AND THEIR PRODUCTION IN EACH BUILDING

Table 8: Complete data obtained for each target University building using Qr6 turbines

Building Number	Building Name	Number turbines	Qr6 turbine			
			Electricity (kWh)	Percentage (%)	Annual savings (£)	Payback Period (years)
1	Lynden House	1	22,343.00	63%	£3,351.45	13.13
2	Maurice Court	9	172,720.47	67%	£25,908.07	15.28
3	Creed Court	6	76,948.23	37%	£11,542.23	22.87
4 and 5	France House	6	159,319.47	42%	£23,897.92	11.05
6	Beaumont Court	7	164,683.03	52%	£24,702.45	12.47
7	Richard Fielden House	4	74,115.42	14%	£11,117.31	15.83
All Buildings combined		34	670,130	38%	£100,519.44	14.88

Table 9: Complete data obtained for each target University building using Qr6 turbines

Building Number	Building Name	Number turbines	Aeolos turbine			
			Electricity (kWh)	Percentage (%)	Annual savings (£)	Payback Period (years)
1	Lynden House	1	6,636.34	19%	£995.45	28.13
2	Maurice Court	9	53,037.76	21%	£7,955.66	31.68
3	Creed Court	6	23,879.59	11%	£3,581.94	46.90
4 and 5	France House	6	68,604.25	18%	£10,290.64	16.33
6	Beaumont Court	7	49,503.24	16%	£7,425.49	26.40
7	Richard Fielden House	4	22,132.57	4%	£3,319.89	33.74
All Buildings combined		34	223,793.76	15%	£33,569.06	28.36